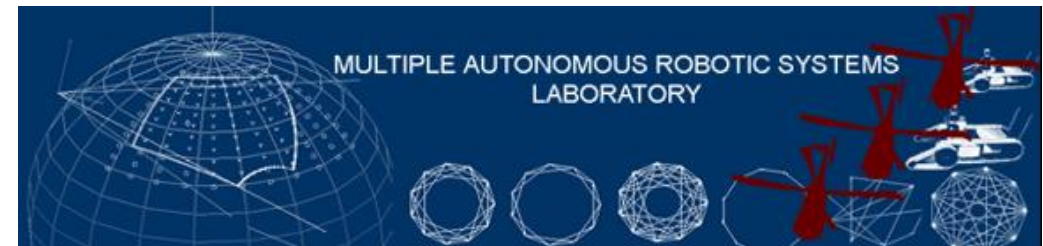


Visual Inertial Navigation Short Tutorial

Stergios Roumeliotis

University of Minnesota

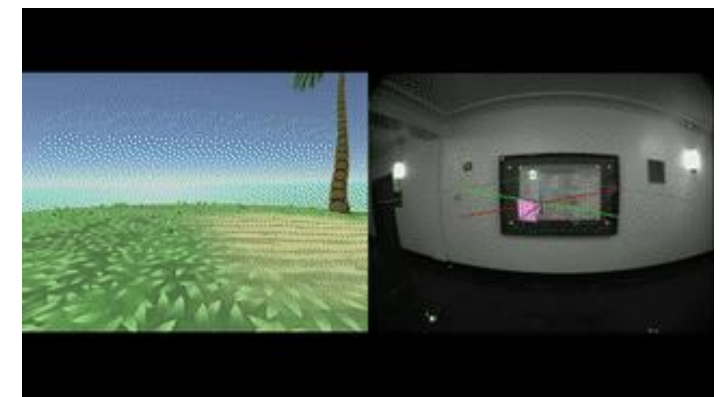
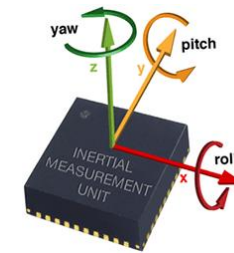


Outline

- VINS Introduction
- IMU/Camera: Models, spatial/temporal calibration
- Image Processing: Feature extraction, tracking, loop closure detection
- VIO/SLAM
 - MSCKF feature classification/processing
 - MSCKF and its (mysterious) relation to optimization methods
 - Observability and inconsistency
- Mapping
 - Offline/online, centralized/distributed approaches
 - Map-based updates and inconsistency
- Interesting Research Directions

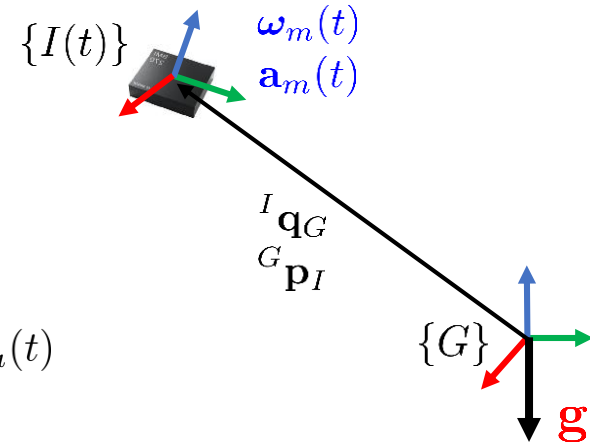
Introduction

- Visual Inertial Navigation Systems (VINS) combine camera and IMU measurements in real time to
 - Determine 6 DOF position & orientation (pose)
 - Create 3D map of surroundings
- Applications
 - Autonomous navigation, augmented/virtual reality



- VINS advantage: IMU-camera complementary sensors -> low cost/high accuracy

IMU Model



- IMU Measurement Model

- Gyroscope: $\boldsymbol{\omega}_m(t) = {}^I\boldsymbol{\omega}(t) + \mathbf{b}_g(t) + \mathbf{n}_g(t)$
- Accelerometer: $\mathbf{a}_m(t) = \mathbf{C}({}^I\mathbf{q}_G(t))({}^G\mathbf{a}(t) - {}^G\mathbf{g}) + \mathbf{b}_a(t) + \mathbf{n}_a(t)$

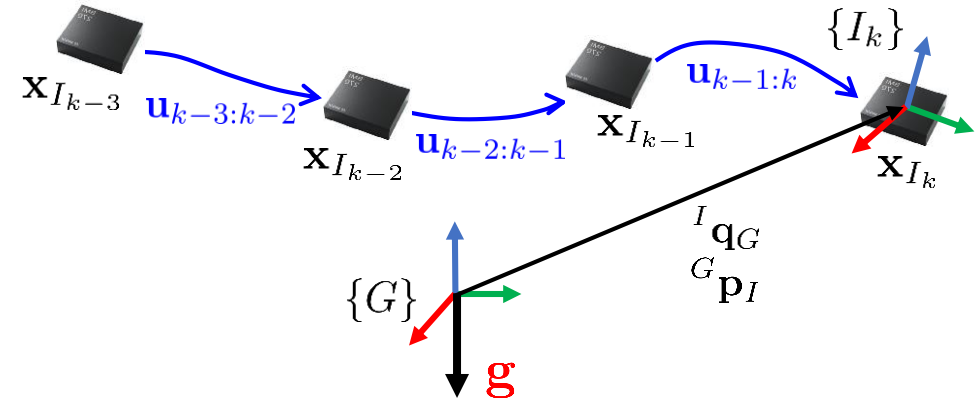
- Continuous-time System Equations

$$\begin{aligned} {}^I\dot{\mathbf{q}}_G(t) &= \frac{1}{2}\boldsymbol{\Omega}(\boldsymbol{\omega}_m(t) - \mathbf{b}_g(t) - \mathbf{n}_g(t)){}^I\mathbf{q}_G(t) \\ \dot{\mathbf{b}}_g(t) &= \mathbf{n}_{wg}(t) \\ {}^G\dot{\mathbf{v}}_I(t) &= \mathbf{C}^T({}^I\mathbf{q}_G(t))(\mathbf{a}_m(t) - \mathbf{b}_a(t) - \mathbf{n}_a(t)) + {}^G\mathbf{g} \\ \dot{\mathbf{b}}_a(t) &= \mathbf{n}_{wa}(t) \\ {}^G\dot{\mathbf{p}}_I(t) &= {}^G\mathbf{v}_I(t) \end{aligned}$$

$$\left. \begin{aligned} & \\ & \\ & \\ & \end{aligned} \right\} \begin{aligned} \dot{\mathbf{x}}_I(t) &= \mathbf{f}_c(\mathbf{x}_I(t), \mathbf{u}(t) - \mathbf{n}(t)) \\ \mathbf{x}_I &= [{}^I\mathbf{q}_G^T \quad \mathbf{b}_g^T \quad {}^G\mathbf{v}_I^T \quad \mathbf{b}_a^T \quad {}^G\mathbf{p}_I^T]^T \\ \mathbf{u}(t) &= [\boldsymbol{\omega}_m(t)^T \quad \mathbf{a}_m(t)^T]^T \end{aligned}$$

- \mathbf{q} : Quaternion of orientation
- \mathbf{C} : Rotation matrix
- \mathbf{P} : Position
- \mathbf{v} : Velocity
- \mathbf{a} : Linear acceleration
- $\boldsymbol{\omega}$: Rotational velocity
- \mathbf{b}_a : Accel biases
- \mathbf{b}_g : Gyro biases
- \mathbf{g} : Gravity
- \mathbf{n}_g : Gyro meas/nt noise
- \mathbf{n}_a : Accel meas/nt noise
- \mathbf{n}_{wg} : Gyro bias process noise
- \mathbf{n}_{wa} : Accel bias process noise

IMU Model



- IMU Measurement Model

- Gyroscope: $\omega_m(t) = {}^I \omega(t) + \mathbf{b}_g(t) + \mathbf{n}_g(t)$
- Accelerometer: $\mathbf{a}_m(t) = \mathbf{C}({}^I \mathbf{q}_G(t))({}^G \mathbf{a}(t) - {}^G \mathbf{g}) + \mathbf{b}_a(t) + \mathbf{n}_a(t)$

- Continuous-time System Equations

$${}^I \dot{\mathbf{q}}_G(t) = \frac{1}{2} \boldsymbol{\Omega}(\omega_m(t) - \mathbf{b}_g(t) - \mathbf{n}_g(t)) {}^I \mathbf{q}_G(t)$$

$$\dot{\mathbf{b}}_g(t) = \mathbf{n}_{wg}(t)$$

$${}^G \dot{\mathbf{v}}_I(t) = \mathbf{C}^T({}^I \mathbf{q}_G(t))(\mathbf{a}_m(t) - \mathbf{b}_a(t) - \mathbf{n}_a(t)) + {}^G \mathbf{g}$$

$$\dot{\mathbf{b}}_a(t) = \mathbf{n}_{wa}(t)$$

$${}^G \dot{\mathbf{p}}_I(t) = {}^G \mathbf{v}_I(t)$$

$$\left. \begin{array}{l} {}^I \dot{\mathbf{q}}_G(t) = \frac{1}{2} \boldsymbol{\Omega}(\omega_m(t) - \mathbf{b}_g(t) - \mathbf{n}_g(t)) {}^I \mathbf{q}_G(t) \\ \dot{\mathbf{b}}_g(t) = \mathbf{n}_{wg}(t) \\ {}^G \dot{\mathbf{v}}_I(t) = \mathbf{C}^T({}^I \mathbf{q}_G(t))(\mathbf{a}_m(t) - \mathbf{b}_a(t) - \mathbf{n}_a(t)) + {}^G \mathbf{g} \\ \dot{\mathbf{b}}_a(t) = \mathbf{n}_{wa}(t) \\ {}^G \dot{\mathbf{p}}_I(t) = {}^G \mathbf{v}_I(t) \end{array} \right\} \begin{array}{l} \dot{\mathbf{x}}_I(t) = \mathbf{f}_c(\mathbf{x}_I(t), \mathbf{u}(t) - \mathbf{n}(t)) \\ \mathbf{x}_I = [{}^I \mathbf{q}_G^T \quad \mathbf{b}_g^T \quad {}^G \mathbf{v}_I^T \quad \mathbf{b}_a^T \quad {}^G \mathbf{p}_I^T]^T \\ \mathbf{u}(t) = [\omega_m(t)^T \quad \mathbf{a}_m(t)^T]^T \end{array}$$

- \mathbf{q} : Quaternion of orientation
- \mathbf{C} : Rotation matrix
- \mathbf{P} : Position
- \mathbf{v} : Velocity
- \mathbf{a} : Linear acceleration
- ω : Rotational velocity
- \mathbf{b}_a : Accel biases
- \mathbf{b}_g : Gyro biases
- \mathbf{g} : Gravity
- \mathbf{n}_g : Gyro meas/nt noise
- \mathbf{n}_a : Accel meas/nt noise
- \mathbf{n}_{wg} : Gyro bias process noise
- \mathbf{n}_{wa} : Accel bias process noise

- IMU Integration [1]

$$\mathbf{x}_{I_k} = \mathbf{f}_d(\mathbf{x}_{I_{k-1}}, \mathbf{u}_{k-1:k}) + \mathbf{n}_k \quad \longrightarrow$$

$$\mathcal{C}_u(\mathbf{x}_{I_{k-1}}, \mathbf{x}_{I_k}) = \|\mathbf{x}_{I_k} - \mathbf{f}_d(\mathbf{x}_{I_{k-1}}, \mathbf{u}_{k-1:k})\|_{\mathbf{Q}_k}^2$$

- IMU Intrinsic [2]

- Accel/gyro scale factors & skewness
- Accel-gyro relative orientation

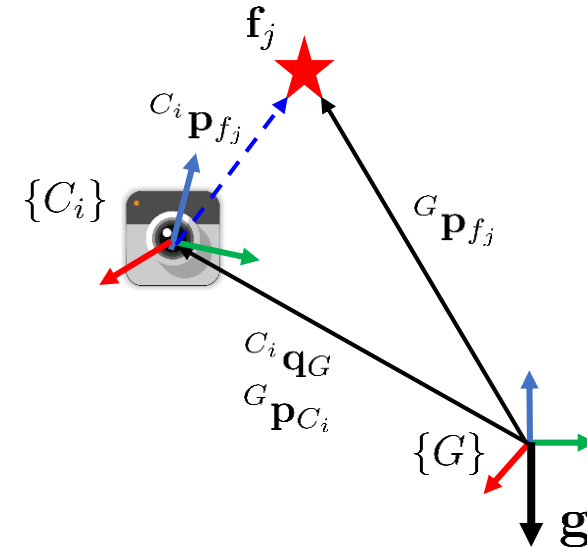
[1] A. I. Mourikis and S. I. Roumeliotis, "A multi-state constraint Kalman filter for vision-aided inertial navigation," ICRA'07

[2] M. Li, H. Yu, X. Zheng, and A. I. Mourikis, "High-fidelity sensor modeling and calibration in vision-aided inertial navigation," ICRA'14

Camera Model

- Camera Measurement Model

$$\mathbf{z}_i^j = \mathbf{h}({}^{C_i}\mathbf{p}_{f_j}) + \mathbf{n}_i^j, \quad {}^{C_i}\mathbf{p}_{f_j} = \mathbf{C}({}^{C_i}\mathbf{q}_G)({}^G\mathbf{p}_{f_j} - {}^G\mathbf{p}_{C_i})$$



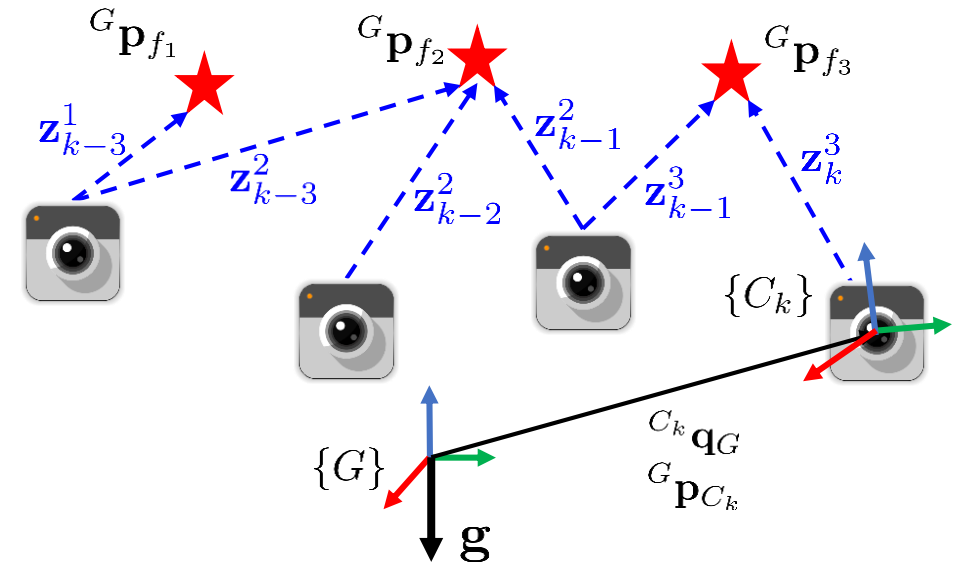
Camera Model

- Camera Measurement Model

$$\mathbf{z}_i^j = \mathbf{h}(\mathbf{C}_i \mathbf{p}_{f_j}) + \mathbf{n}_i^j, \quad \mathbf{C}_i \mathbf{p}_{f_j} = \mathbf{C}(\mathbf{C}_i \mathbf{q}_G)(\mathbf{G} \mathbf{p}_{f_j} - \mathbf{G} \mathbf{p}_{C_i})$$

- Camera Intrinsics

- Principal point & focal length
- Distortion parameters
- Rolling-shutter time



Distorted image



Geometry change

Camera-IMU Model

- Camera Measurement Model

$$\mathbf{z}_i^j = \mathbf{h}({}^{C_i}\mathbf{p}_{f_j}) + \mathbf{n}_i^j, \quad {}^{C_i}\mathbf{p}_{f_j} = \mathbf{C}({}^{C_i}\mathbf{q}_G)({}^G\mathbf{p}_{f_j} - {}^G\mathbf{p}_{C_i})$$

- Camera Intrinsics

- Principal point & focal length
- Distortion parameters
- Rolling-shutter time

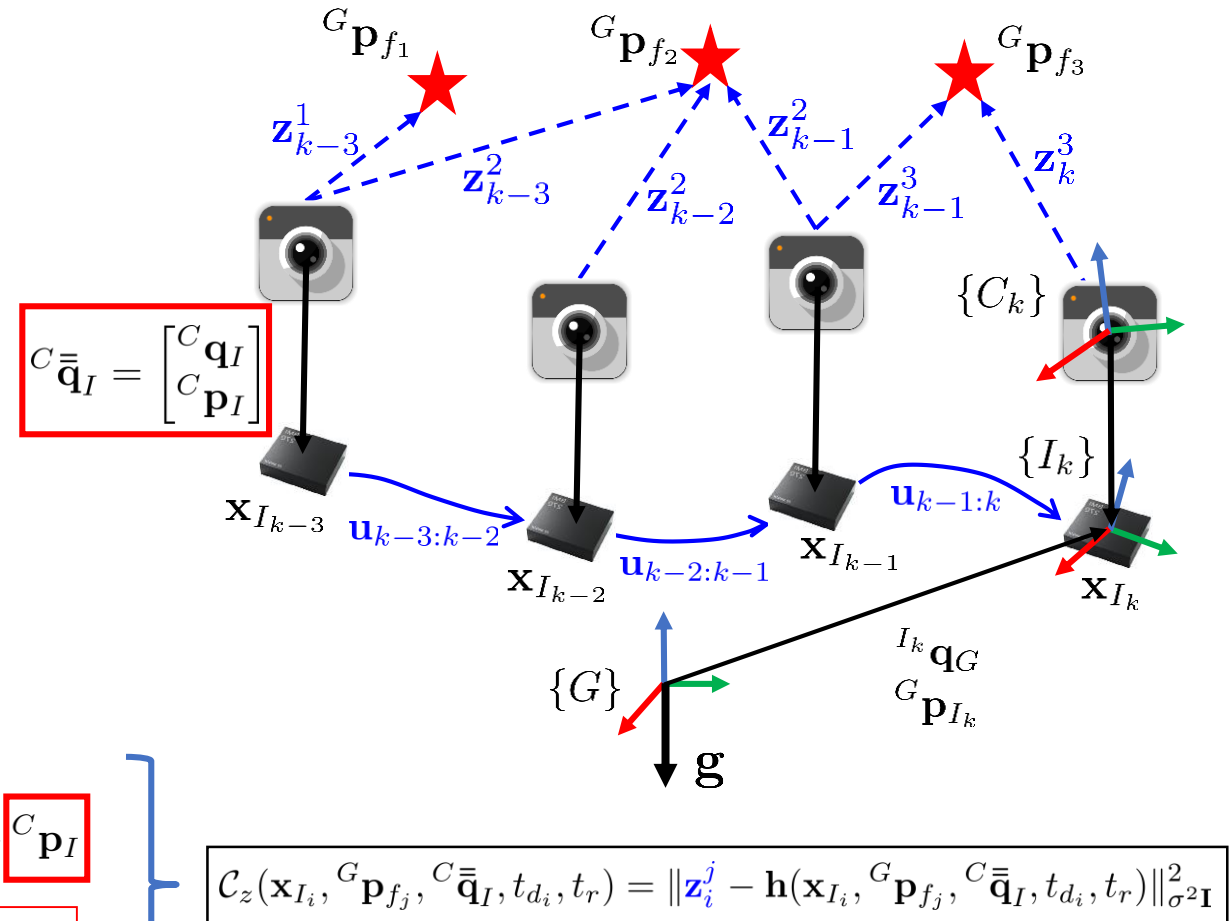
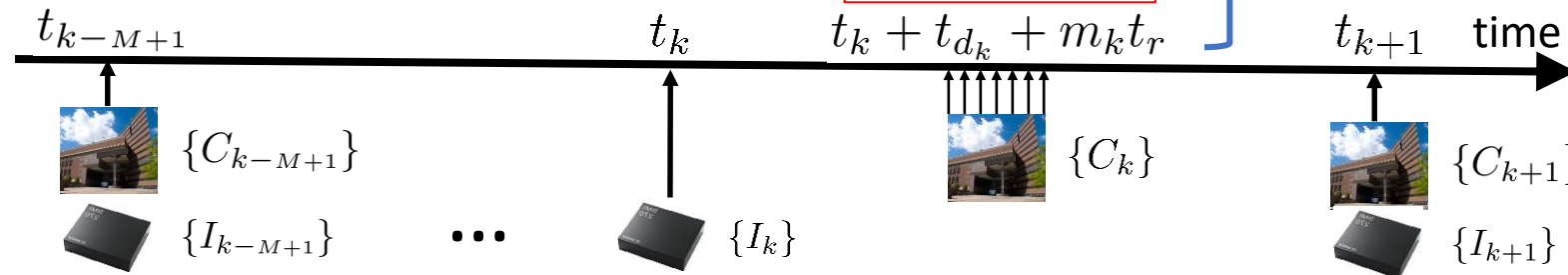
- Camera-IMU Extrinsic

- Spatial: Rigid-body transformation [1]

$${}^{C_i}\mathbf{p}_{f_j} = \frac{{}^{C_i}}{G}\mathbf{C}({}^G\mathbf{p}_{f_j} - {}^G\mathbf{p}_{C_i}) = \mathbf{C}({}^{C_i}\mathbf{q}_G) \frac{{}^{C_i}}{G}\mathbf{C}({}^G\mathbf{p}_{f_j} - {}^G\mathbf{p}_{I_i}) + \mathbf{C}({}^{C_i}\mathbf{p}_I)$$

- Temporal: Time offset [2]

RS/TS effect



$$\mathcal{C}_z(\mathbf{x}_{I_i}, {}^G\mathbf{p}_{f_j}, {}^{C_i}\mathbf{q}_I, t_{d_i}, t_r) = \|\mathbf{z}_i^j - \mathbf{h}(\mathbf{x}_{I_i}, {}^G\mathbf{p}_{f_j}, {}^{C_i}\mathbf{q}_I, t_{d_i}, t_r)\|_{\sigma^2\mathbf{I}}^2$$

[1] F. M. Mirzaei and S. I. Roumeliotis, "A Kalman Filter-based Algorithm for IMU-Camera Calibration: Observability Analysis and Performance Evaluation," TRO'08

[2] C. Guo, D. G. Kottas, R. DuToit, A. Ahmed, R. Li, and S. I. Roumeliotis, "Efficient visual-inertial navigation using a rolling-shutter camera with inaccurate timestamps," RSS'14

Feature Extraction & Tracking

- Keypoint detection
 - Harris ^[1], DoG, FAST ^[2]



[1] C. Harris and M. Stephens, "A Combined Corner and Edge Detector," Alvey Vision Conference'81

[2] R. Edward and T. Drummond, "Machine learning for high-speed corner detection," ECCV'06

Feature Extraction & Tracking

- Keypoint detection
 - Harris [1], DoG, FAST [2]
- Descriptor extraction
 - SIFT [3], SURF [4], ORB [5], FREAK [6], BRISK [7], SDC [8]

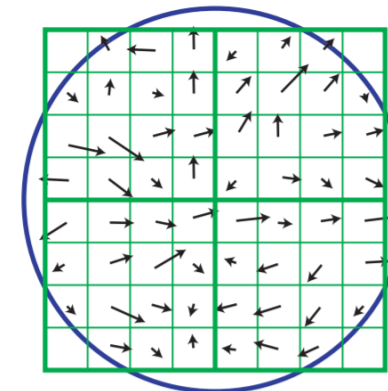
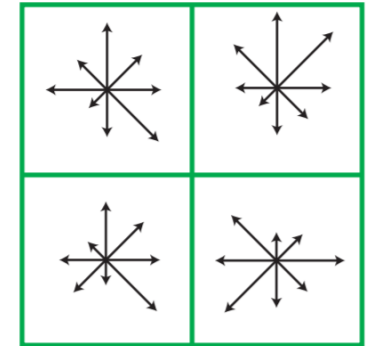
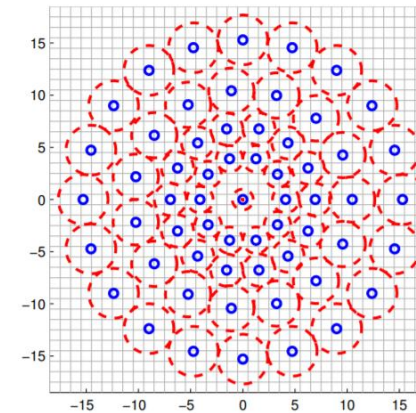


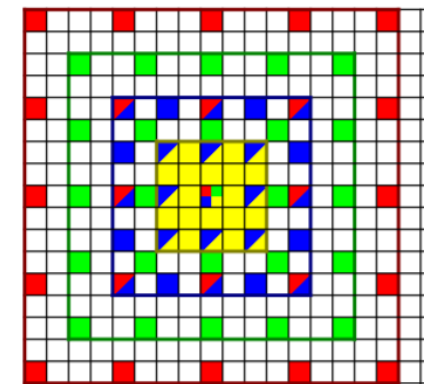
Image gradients



Keypoint descriptor



BRISK



SDC

[3] D. Lowe, “Distinctive Image Features from Scale-Invariant Keypoints,” IJCV’04

[4] H. Bay, A. Ess, T. Tuytelaars, and L. Van Gool, “Speeded-up robust features (SURF),” Computer Vision and Image Understanding’08

[5] E. Rublee, V. Rabaud, K. Konolige, and G. Bradski, “ORB: An efficient alternative to SIFT or SURF,” ICCV’11

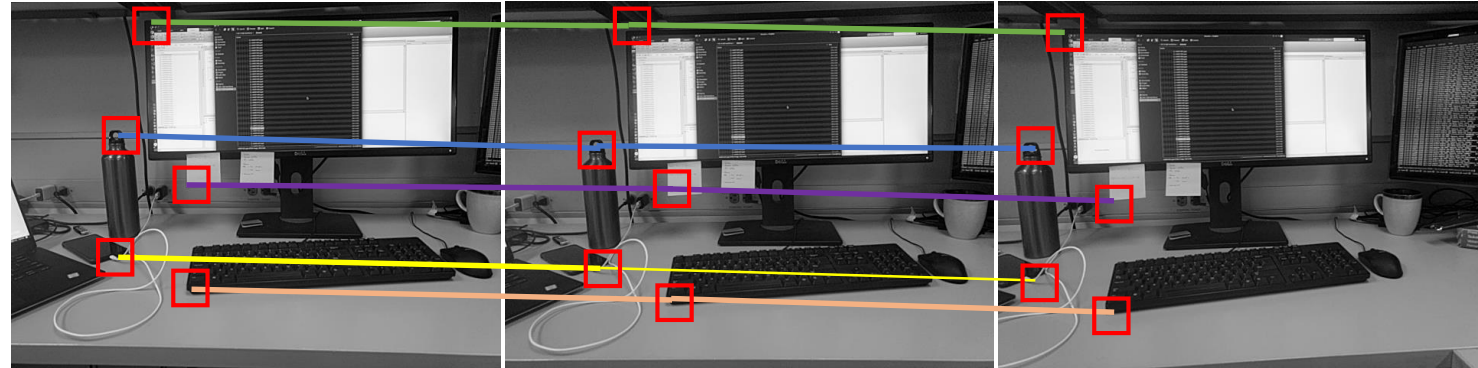
[6] A. Alahi, R. Ortiz, Raphael, and P. Vandergheynst, “FREAK: Fast Retina Keypoint,” CVPR’12

[7] S. Leutenegger, M. Chli, and R. Siegwart, “BRISK: Binary robust invariant scalable keypoints,” ICCV’11

[8] R. Schuster, O. Wasenmuller, C. Unger, and D. Stricker, “SDC – Stacked Dilated Convolution: A Unified Descriptor Network for Dense Matching,” CVPR’19

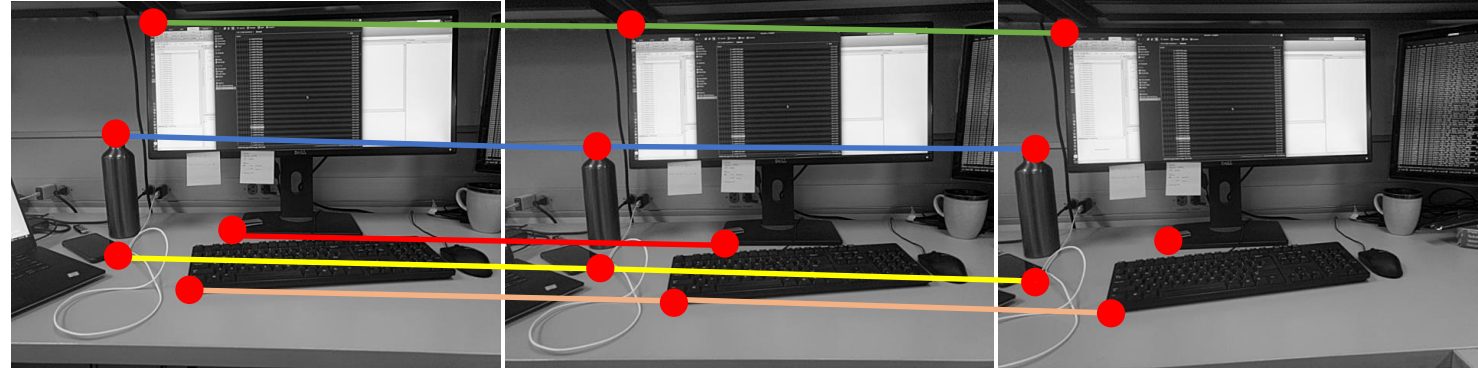
Feature Extraction & Tracking

- Keypoint detection
 - Harris ^[1], DoG, FAST ^[2]
- Descriptor extraction
 - SIFT ^[3], SURF ^[4], ORB ^[5], FREAK ^[6], BRISK ^[7], SDC ^[8]
- Feature tracking (2D-to-2D)
 - KLT ^[9]



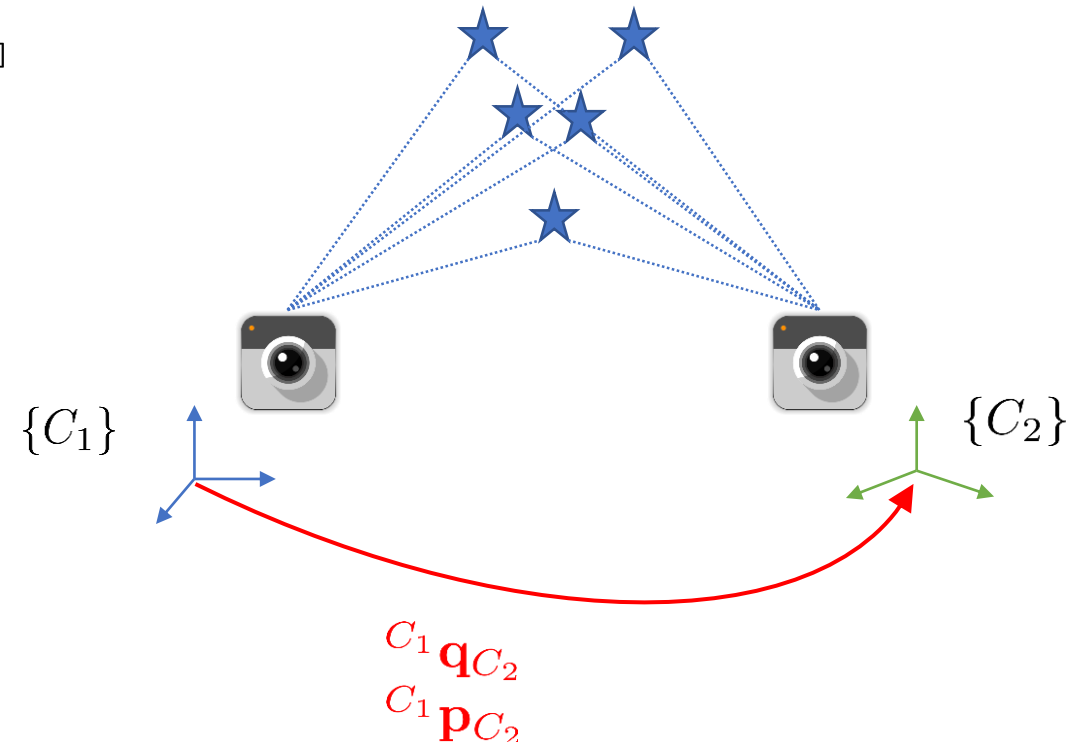
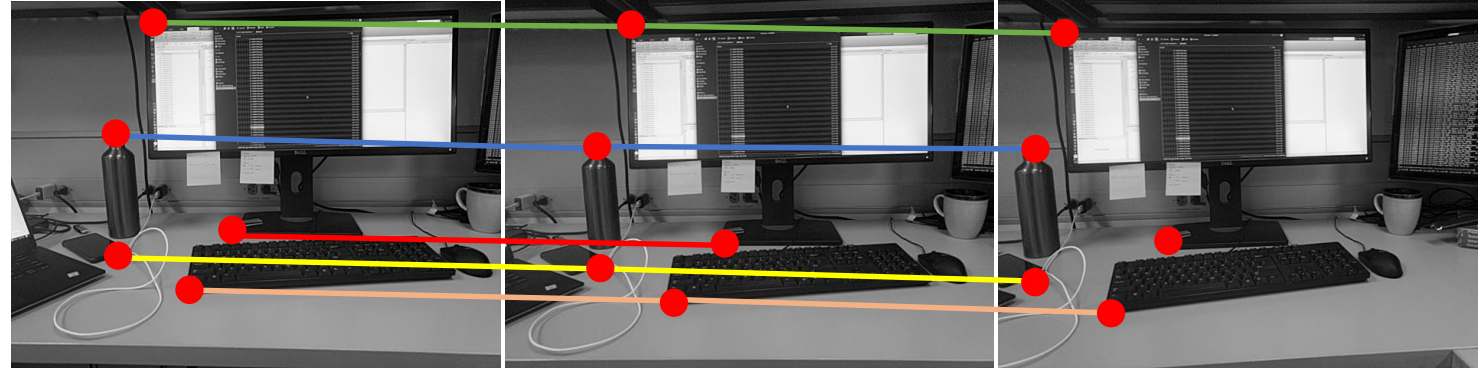
Feature Extraction & Tracking

- Keypoint detection
 - Harris ^[1], DoG, FAST ^[2]
- Descriptor extraction
 - SIFT ^[3], SURF ^[4], ORB ^[5], FREAK ^[6], BRISK ^[7], SDC ^[8]
- Feature tracking (2D-to-2D)
 - KLT ^[9]
 - Descriptor-to-descriptor matching



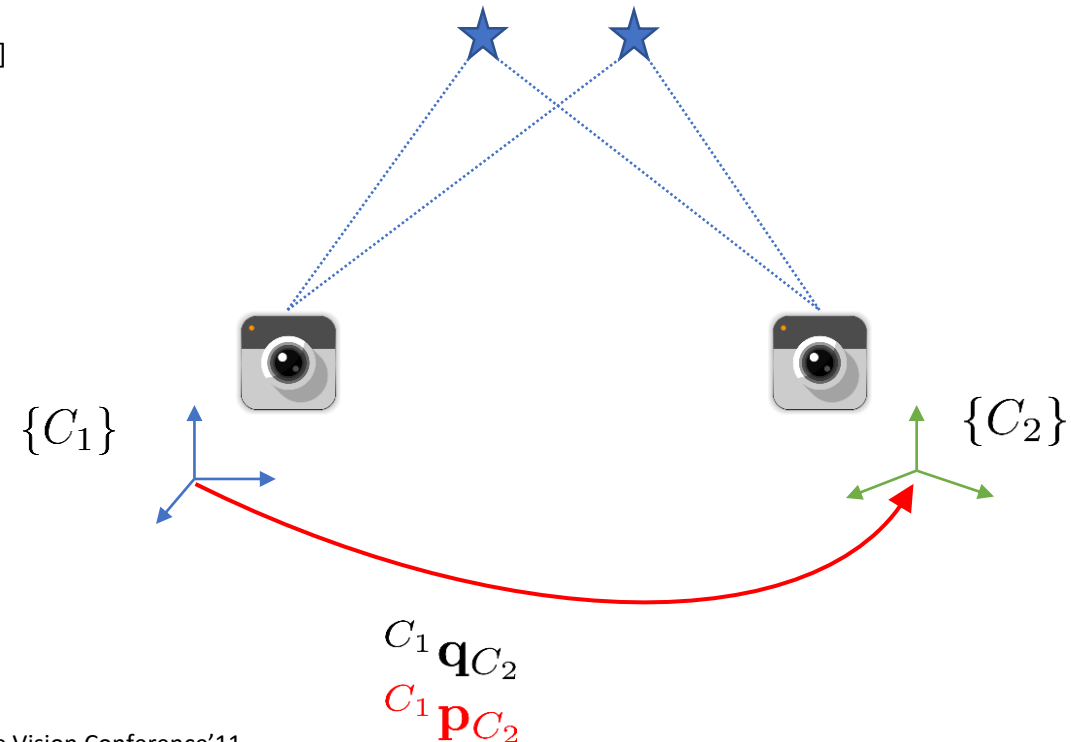
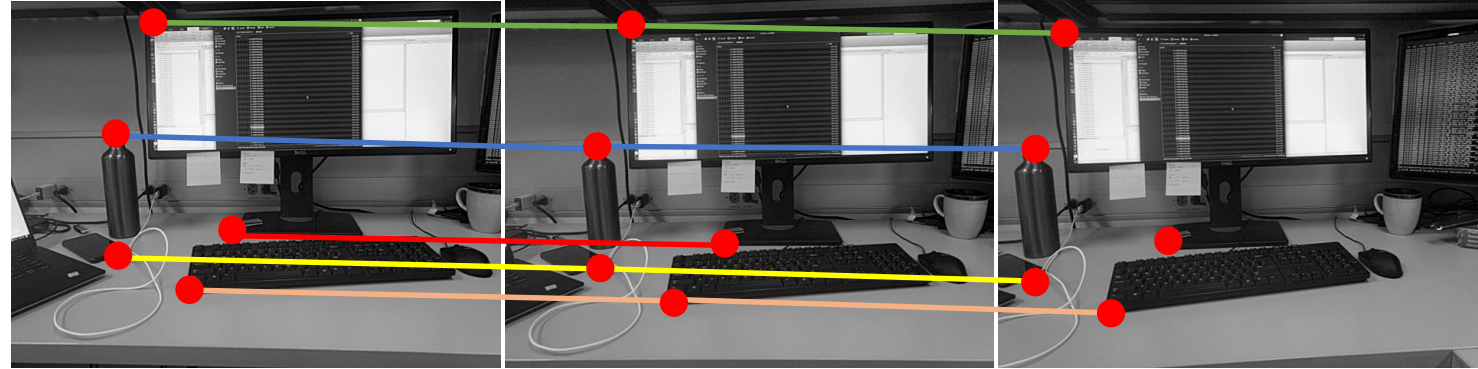
Feature Extraction & Tracking

- Keypoint detection
 - Harris [1], DoG, FAST [2]
- Descriptor extraction
 - SIFT [3], SURF [4], ORB [5], FREAK [6], BRISK [7], SDC [8]
- Feature tracking (2D-to-2D)
 - KLT [9]
 - Descriptor-to-descriptor matching
 - Outlier rejection (RANSAC)
 - w/out gyro: 5pt RANSAC [10]



Feature Extraction & Tracking

- Keypoint detection
 - Harris [1], DoG, FAST [2]
- Descriptor extraction
 - SIFT [3], SURF [4], ORB [5], FREAK [6], BRISK [7], SDC [8]
- Feature tracking (2D-to-2D)
 - KLT [9]
 - Descriptor-to-descriptor matching
 - Outlier rejection (RANSAC)
 - w/out gyro: 5pt RANSAC [10]
 - w/ gyro: 2pt RANSAC [11]

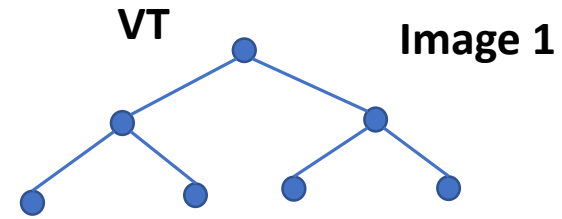


[10] D. Nister, "An efficient solution to the five-point relative pose problem," TPAMI'04

[11] L. Kneip, M. Chli, and R. Siegwart, "Robust real-time visual odometry with a single camera and an IMU," British Machine Vision Conference'11

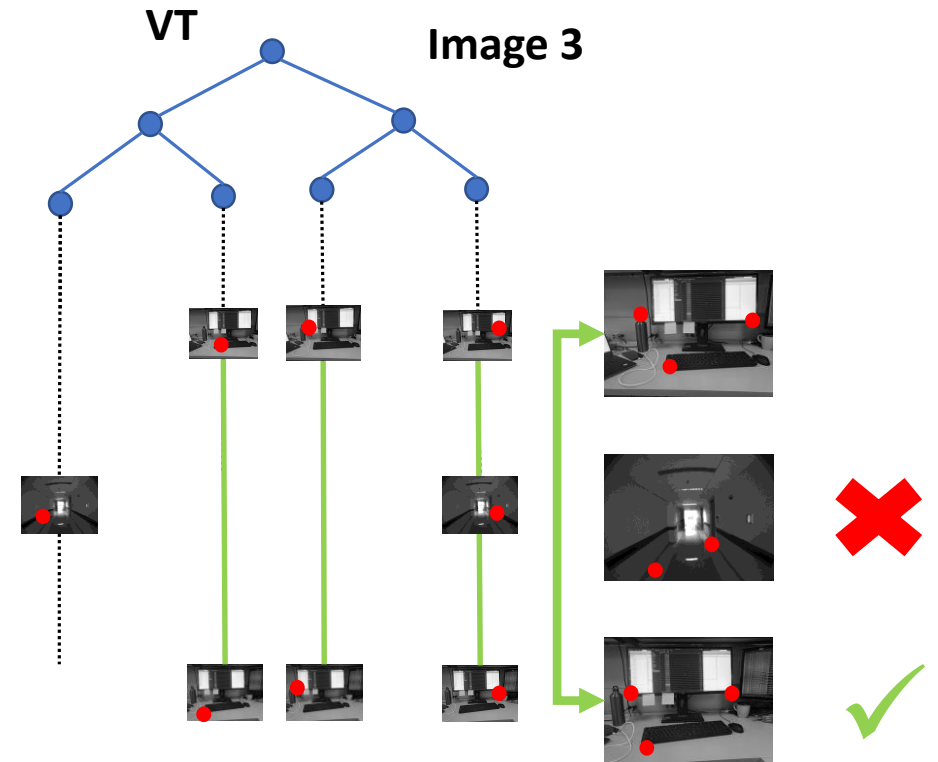
Loop-closure Detection

- Appearance-based image matching ^[1]
 - Create image descriptor from feature descriptors
 - Compare image descriptors against each other



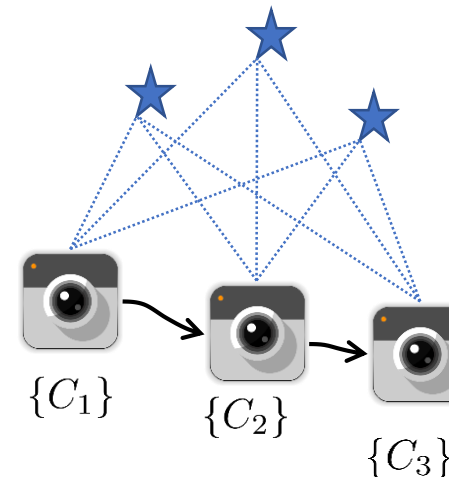
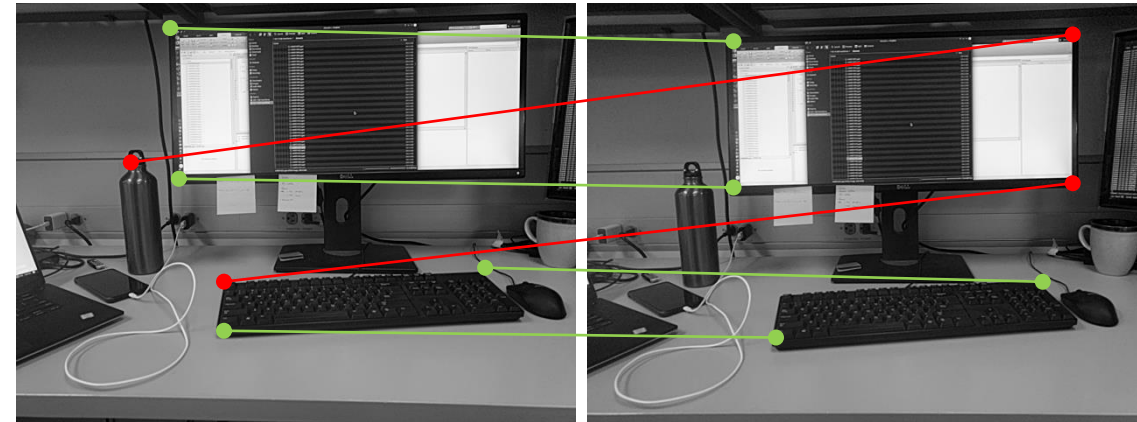
Loop-closure Detection

- Appearance-based image matching [1]
 - Create image descriptor from feature descriptors
 - Compare image descriptors against each other



Loop-closure Detection

- Appearance-based image matching ^[1]
 - Create image descriptor from feature descriptors
 - Compare image descriptors against each other
- Outlier rejection / Geometric verification
 - 5pt_[2] (3pt+1_[3]) RANSAC to verify 2D-2D matches
 - P3P_[4] (P2+1_[5]) RANSAC for 2D-3D matches
 - Confirm loop-closure by matching consecutive images
 - Reduces false-positives
 - Delays map-based updates



[2] D. Nister, "An efficient solution to the five-point relative pose problem," TPAMI'04

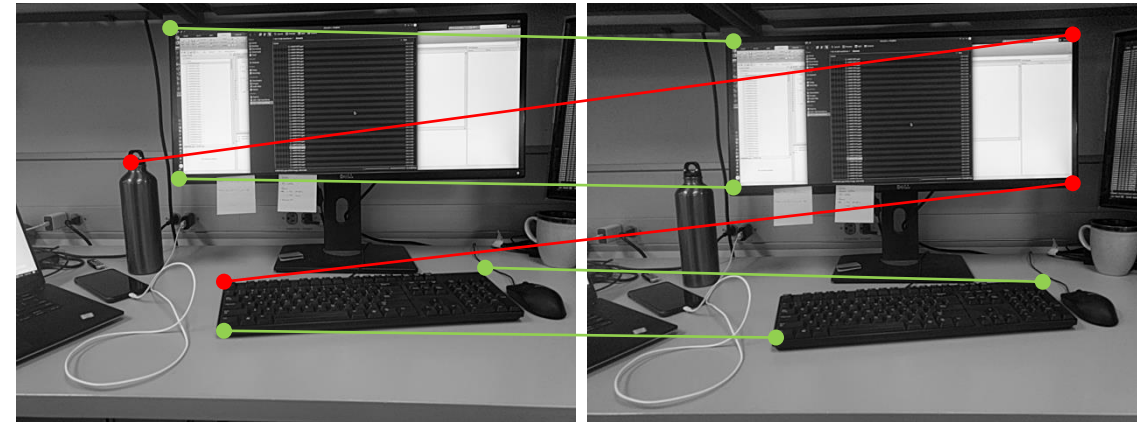
[3] O. Naroditsky, X. Zhou, S. Roumeliotis, and K. Daniilidis, "Two efficient solutions for visual odometry using directional correspondence," TPAMI'12

[4] T. Ke, S. Roumeliotis, "An Efficient Algebraic Solution to the Perspective-Three-Point Problem," CVPR'17

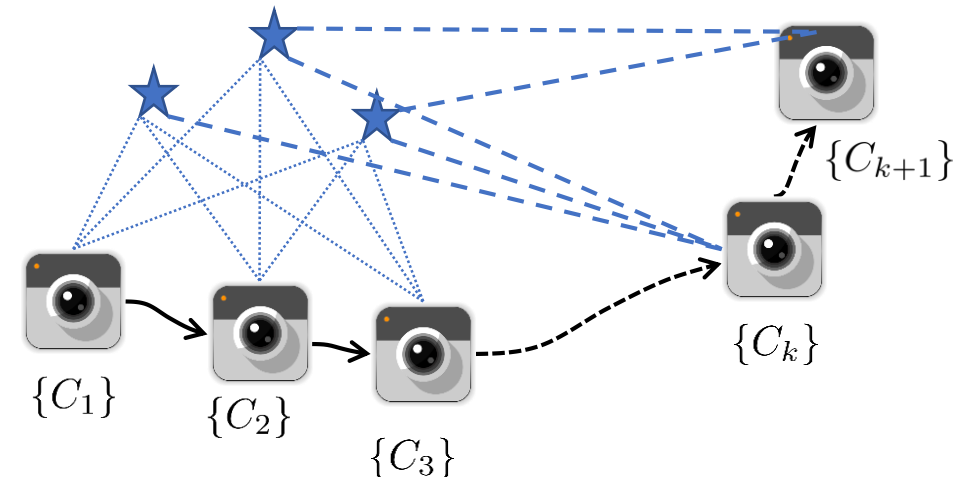
[5] Z. Kukelova, M. Bujnak, and T. Pajdla, "Closed-form solutions to minimal absolute pose problems with known vertical direction," ACCV'11

Loop-closure Detection

- Appearance-based image matching ^[1]
 - Create image descriptor from feature descriptors
 - Compare image descriptors against each other
- Outlier rejection / Geometric verification
 - 5pt_[2] (3pt+1_[3]) RANSAC to verify 2D-2D matches
 - P3P_[4] (P2+1_[5]) RANSAC for 2D-3D matches
 - Confirm loop-closure by matching consecutive images
 - Reduces false-positives
 - Delays map-based updates



LC



[2] D. Nister, "An efficient solution to the five-point relative pose problem," TPAMI'04

[3] O. Naroditsky, X. Zhou, S. Roumeliotis, and K. Daniilidis, "Two efficient solutions for visual odometry using directional correspondence," TPAMI'12

[4] T. Ke, S. Roumeliotis, "An Efficient Algebraic Solution to the Perspective-Three-Point Problem," CVPR'17

[5] Z. Kukelova, M. Bujnak, and T. Pajdla, "Closed-form solutions to minimal absolute pose problems with known vertical direction," ACCV'11

Sensor (IMU+Camera) Fusion

- Incremental BLS optimization_[1]

$$\mathcal{C}_N = \sum_{k=1}^N \|\mathbf{x}_{I_k} - \mathbf{f}(\mathbf{x}_{I_{k-1}}, \mathbf{u}_{k-1:k})\|_{\mathbf{Q}_k}^2 + \sum_{k=1}^N \sum_j \|\mathbf{z}_k^j - \mathbf{h}(\mathbf{x}_{I_k}, {}^G \mathbf{p}_{f_j})\|_{\sigma^2 \mathbf{I}}^2$$

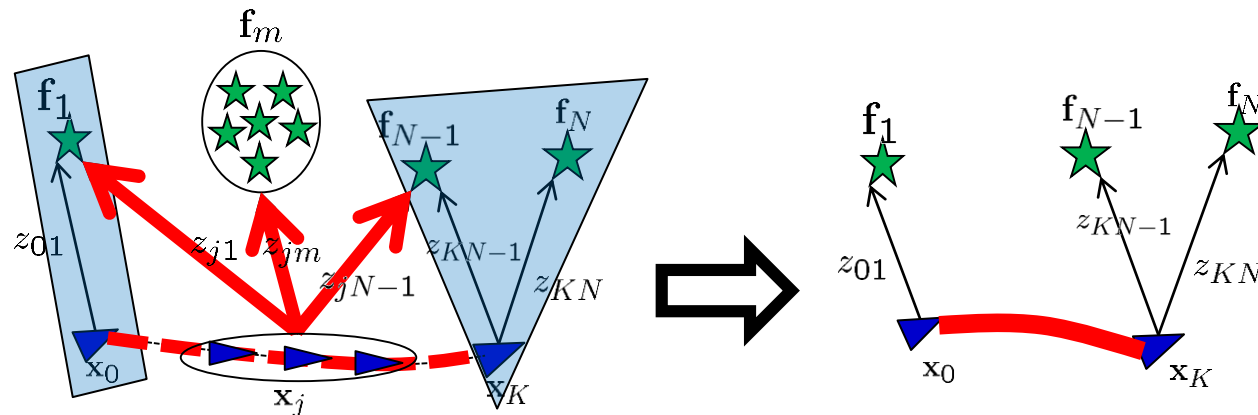
- Issue: Memory/CPU req.s increase w/ time

Sensor (IMU+Camera) Fusion

- Incremental BLS optimization_[1]

$$C_N = \sum_{k=1}^N \|\mathbf{x}_{I_k} - \mathbf{f}(\mathbf{x}_{I_{k-1}}, \mathbf{u}_{k-1:k})\|_{\mathbf{Q}_k}^2 + \sum_{k=1}^N \sum_j \|\mathbf{z}_k^j - \mathbf{h}(\mathbf{x}_{I_k}, {}^G \mathbf{p}_{f_j})\|_{\sigma^2 \mathbf{I}}^2$$

- Issue: Memory/CPU req.s increase w/ time
- Remedy: C-KLAM_[2] consistently marginalizes keyframes/features

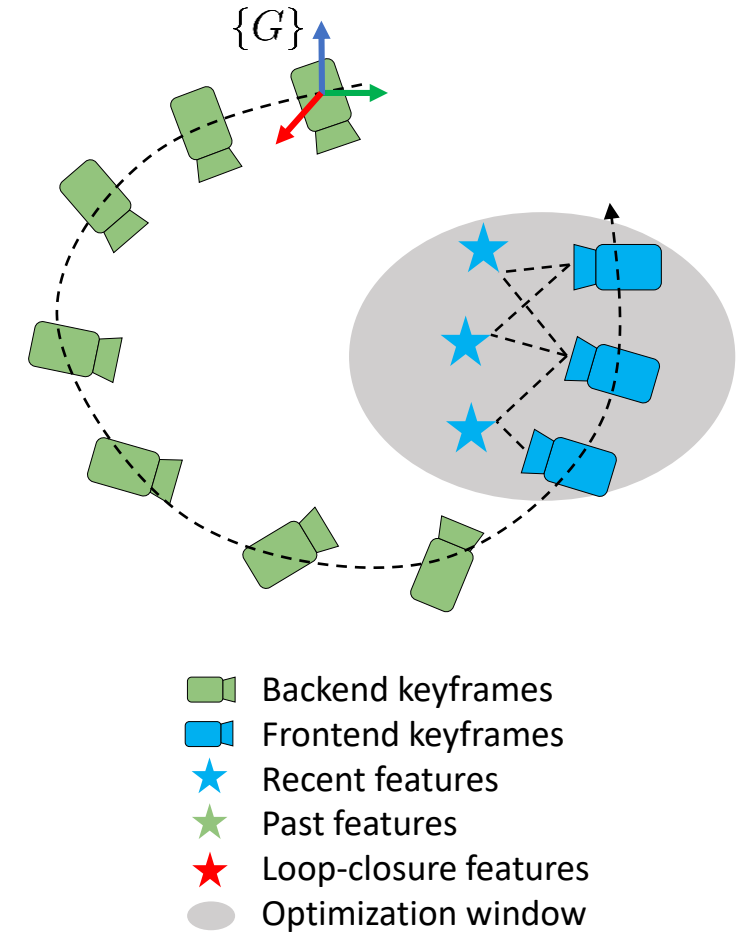


Sensor (IMU+Camera) Fusion

- Incremental BLS optimization_[1]

$$\mathcal{C}_N = \sum_{k=1}^N \|\mathbf{x}_{I_k} - \mathbf{f}(\mathbf{x}_{I_{k-1}}, \mathbf{u}_{k-1:k})\|_{\mathbf{Q}_k}^2 + \sum_{k=1}^N \sum_j \|\mathbf{z}_k^j - \mathbf{h}(\mathbf{x}_{I_k}, {}^G \mathbf{p}_{f_j})\|_{\sigma^2 \mathbf{I}}^2$$

- Issue: Memory/CPU req.s increase w/ time
- Alternative VINS approach
 - Split the problem into
 - Frontend (Localization): Fast, but drifts w/ time
 - e.g., Visual Inertial Odometry (VIO)

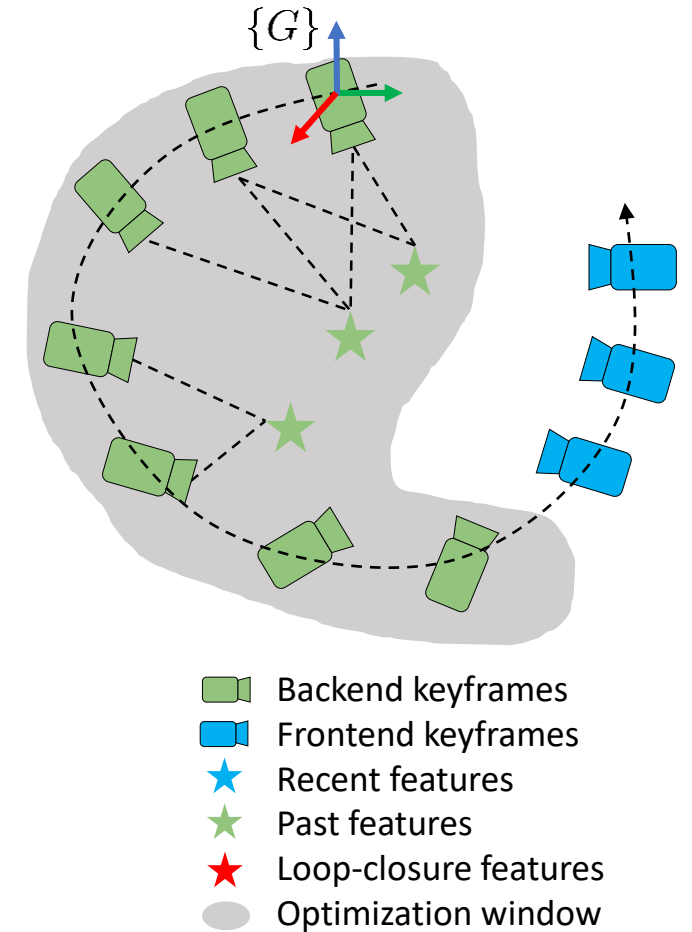


Sensor (IMU+Camera) Fusion

- Incremental BLS optimization_[1]

$$\mathcal{C}_N = \sum_{k=1}^N \|\mathbf{x}_{I_k} - \mathbf{f}(\mathbf{x}_{I_{k-1}}, \mathbf{u}_{k-1:k})\|_{\mathbf{Q}_k}^2 + \sum_{k=1}^N \sum_j \|\mathbf{z}_k^j - \mathbf{h}(\mathbf{x}_{I_k}, {}^G \mathbf{p}_{f_j})\|_{\sigma^2 \mathbf{I}}^2$$

- Issue: Memory/CPU req.s increase w/ time
- Alternative VINS approach
 - Split the problem into
 - Frontend (Localization): Fast, but drifts w/ time
 - e.g., Visual Inertial Odometry (VIO)
 - Backend (Mapping): Slow, but more accurate
 - e.g., BLS, pose graph

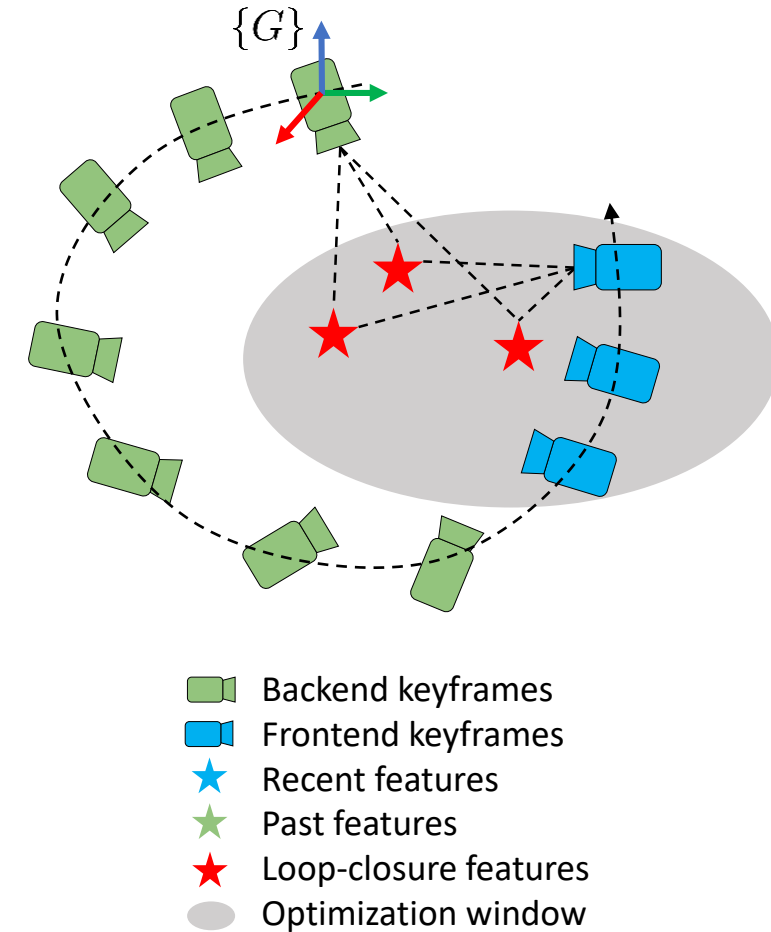


Sensor (IMU+Camera) Fusion

- Incremental BLS optimization_[1]

$$\mathcal{C}_N = \sum_{k=1}^N \|\mathbf{x}_{I_k} - \mathbf{f}(\mathbf{x}_{I_{k-1}}, \mathbf{u}_{k-1:k})\|_{\mathbf{Q}_k}^2 + \sum_{k=1}^N \sum_j \|\mathbf{z}_k^j - \mathbf{h}(\mathbf{x}_{I_k}, {}^G \mathbf{p}_{f_j})\|_{\sigma^2 \mathbf{I}}^2$$

- Issue: Memory/CPU req.s increase w/ time
- Alternative VINS approach
 - Split the problem into
 - Frontend (Localization): Fast, but drifts w/ time
 - e.g., Visual Inertial Odometry (VIO)
 - Backend (Mapping): Slow, but more accurate
 - e.g., BLS, pose graph
 - Relocalize w/ loop closures
 - Assumes keyframes of backend as perfectly known -> inconsistency
 - Estimated covariance < true covariance



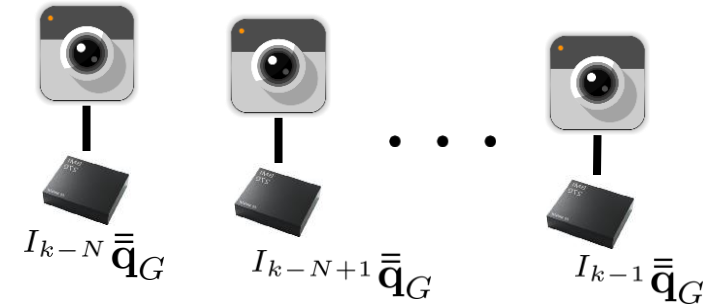
Frontend: Multi-state Constraint Kalman Filter (MSCKF) [1]

- State Vector

$$\mathbf{x}_k = [\mathbf{x}_{I_k} \quad \mathbf{x}_{I_{k-1}} \quad I_{k-2} \bar{\mathbf{q}}_G \dots I_{k-N} \bar{\mathbf{q}}_G \quad C \bar{\mathbf{q}}_I]^T$$

$$\text{where } \mathbf{x}_I = [{}^I \mathbf{q}_G^T \quad \mathbf{b}_g^T \quad {}^G \mathbf{v}_I^T \quad \mathbf{b}_a^T \quad {}^G \mathbf{p}_I^T]^T$$

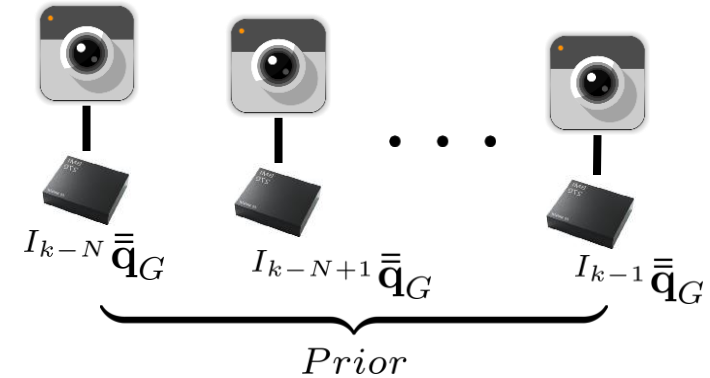
$${}^I \bar{\mathbf{q}}_G = [{}^I \mathbf{q}_G^T \quad {}^G \mathbf{p}_I^T]^T$$



Frontend: Multi-state Constraint Kalman Filter (MSCKF) [1]

- Step 1: Propagation

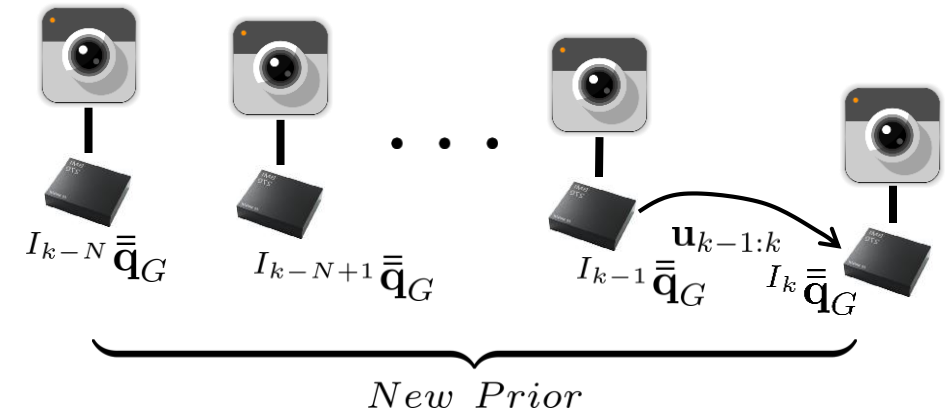
$$C_{k|k-1} = \underbrace{\|\tilde{\mathbf{x}}_{k-1}\|_{\mathbf{P}_{k-1|k-1}}^2}_{\text{Prior}} + \underbrace{\|\mathbf{x}_{I_k} - \mathbf{f}(\mathbf{x}_{I_{k-1}}, \mathbf{u}_{k-1:k})\|_{\mathbf{Q}_k}^2}_{\text{IMU}}$$



Frontend: Multi-state Constraint Kalman Filter (MSCKF) [1]

- Step 1: Propagation

$$\mathcal{C}_{k|k-1} = \underbrace{\|\tilde{\mathbf{x}}_{k-1}\|_{\mathbf{P}_{k-1|k-1}}^2}_{\text{Prior}} + \underbrace{\|\mathbf{x}_{I_k} - \mathbf{f}(\mathbf{x}_{I_{k-1}}, \mathbf{u}_{k-1:k})\|_{\mathbf{Q}_k}^2}_{\text{IMU}}$$
$$\mathcal{C}_{k|k-1} \simeq \underbrace{\|\tilde{\mathbf{x}}_k\|_{\mathbf{P}_{k|k-1}}^2}_{\text{New Prior}}$$



Frontend: Multi-state Constraint Kalman Filter (MSCKF) ^[1]

- Step 1: Propagation

$$\mathcal{C}_{k|k-1} = \underbrace{\|\tilde{\mathbf{x}}_{k-1}\|_{\mathbf{P}_{k-1|k-1}}^2}_{\text{Prior}} + \underbrace{\|\mathbf{x}_{I_k} - \mathbf{f}(\mathbf{x}_{I_{k-1}}, \mathbf{u}_{k-1:k})\|_{\mathbf{Q}_k}^2}_{\text{IMU}}$$

$$\mathcal{C}_{k|k-1} \simeq \underbrace{\|\tilde{\mathbf{x}}_k\|_{\mathbf{P}_{k|k-1}}^2}_{\text{New Prior}}$$

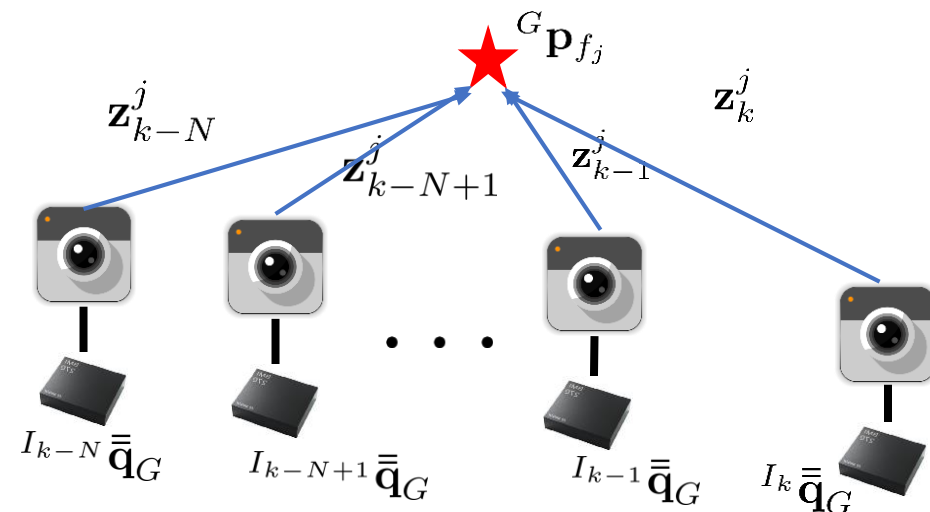
- Step 2: Marginalize all features $[O(N)]$

$$\mathcal{C}_{k|k} = \|\tilde{\mathbf{x}}_k\|_{\mathbf{P}_{k|k-1}}^2 + \sum_j \|\mathbf{z}_{k-N:k}^j - \mathbf{f}(\mathbf{x}_{k-N:k}, \mathbf{p}_{f_j})\|^2$$

$$\simeq \|\tilde{\mathbf{x}}_k\|_{\mathbf{P}_{k|k-1}}^2 + \sum_j \|\tilde{\mathbf{z}}_{k-N:k}^j - (\mathbf{H}_x^j \tilde{\mathbf{x}}_{k-N:k} + \mathbf{H}_f^j \tilde{\mathbf{p}}_{f_j})\|^2$$

$$= \|\tilde{\mathbf{x}}_k\|_{\mathbf{P}_{k|k-1}}^2 + \sum_j \left(\|\mathbf{U}_j^T \tilde{\mathbf{z}}_{k-N:k}^j - \mathbf{U}_j^T \mathbf{H}_x^j \tilde{\mathbf{x}}_{k-N:k}\|^2 + \|\mathbf{V}_j^T \tilde{\mathbf{z}}_{k-N:k}^j - (\mathbf{V}_j^T \mathbf{H}_x^j \tilde{\mathbf{x}}_{k-N:k} + \mathbf{V}_j^T \mathbf{H}_f^j \tilde{\mathbf{p}}_{f_j})\|^2 \right)$$

where $[\mathbf{V}_j \quad \mathbf{U}_j]^T [\mathbf{V}_j \quad \mathbf{U}_j] = \mathbf{I}$, $\mathbf{U}_j^T \mathbf{H}_f^j = \mathbf{0}$



Frontend: Multi-state Constraint Kalman Filter (MSCKF) ^[1]

- Step 1: Propagation

$$\mathcal{C}_{k|k-1} = \underbrace{\|\tilde{\mathbf{x}}_{k-1}\|_{\mathbf{P}_{k-1|k-1}}^2}_{\text{Prior}} + \underbrace{\|\mathbf{x}_{I_k} - \mathbf{f}(\mathbf{x}_{I_{k-1}}, \mathbf{u}_{k-1:k})\|_{\mathbf{Q}_k}^2}_{\text{IMU}}$$

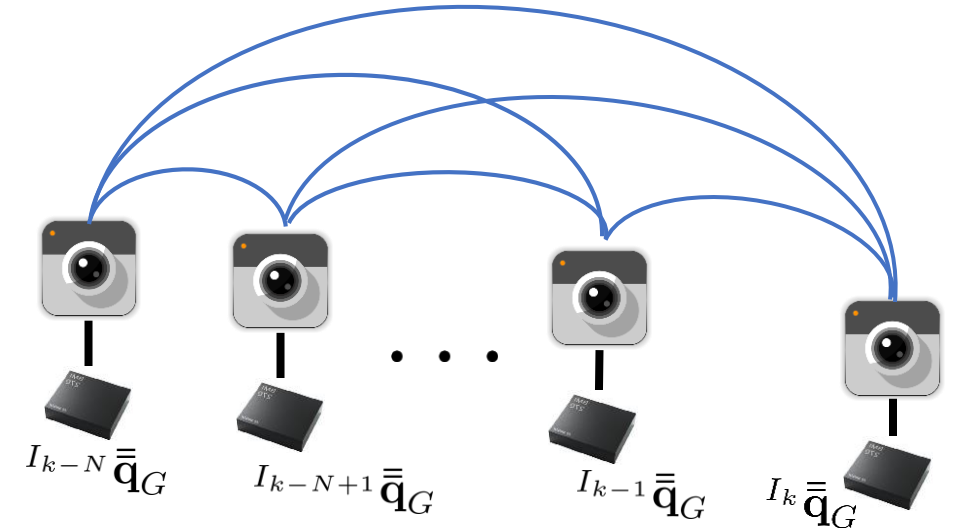
$$\mathcal{C}_{k|k-1} \simeq \underbrace{\|\tilde{\mathbf{x}}_k\|_{\mathbf{P}_{k|k-1}}^2}_{\text{New Prior}}$$

- Step 2: Marginalize all features $[O(N)]$

$$\begin{aligned} \mathcal{C}_{k|k} &= \|\tilde{\mathbf{x}}_k\|_{\mathbf{P}_{k|k-1}}^2 + \sum_j \|\mathbf{z}_{k-N:k}^j - \mathbf{f}(\mathbf{x}_{k-N:k}, \mathbf{p}_{f_j})\|^2 \\ &\simeq \|\tilde{\mathbf{x}}_k\|_{\mathbf{P}_{k|k-1}}^2 + \sum_j \|\tilde{\mathbf{z}}_{k-N:k}^j - (\mathbf{H}_x^j \tilde{\mathbf{x}}_{k-N:k} + \mathbf{H}_f^j \tilde{\mathbf{p}}_{f_j})\|^2 \end{aligned}$$

$$= \|\tilde{\mathbf{x}}_k\|_{\mathbf{P}_{k|k-1}}^2 + \sum_j \left(\|\mathbf{U}_j^T \tilde{\mathbf{z}}_{k-N:k}^j - \mathbf{U}_j^T \mathbf{H}_x^j \tilde{\mathbf{x}}_{k-N:k}\|^2 + \|\mathbf{V}_j^T \tilde{\mathbf{z}}_{k-N:k}^j - (\mathbf{V}_j^T \mathbf{H}_x^j \tilde{\mathbf{x}}_{k-N:k} + \mathbf{V}_j^T \mathbf{H}_f^j \tilde{\mathbf{p}}_{f_j})\|^2 \right)$$

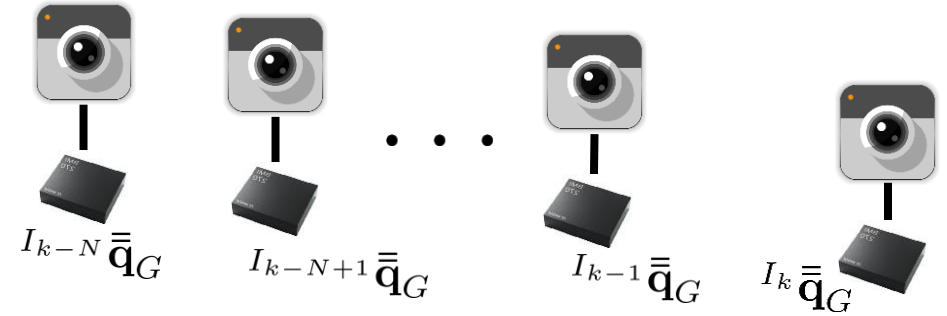
$$\begin{aligned} \mathcal{C}'_{k|k} &= \|\tilde{\mathbf{x}}_k\|_{\mathbf{P}_{k|k-1}}^2 + \sum_j \|\mathbf{U}_j^T \tilde{\mathbf{z}}_{k-N:k}^j - \mathbf{U}_j^T \mathbf{H}_x^j \tilde{\mathbf{x}}_{k-N:k}\|^2 \quad \text{where } [\mathbf{V}_j \quad \mathbf{U}_j]^T [\mathbf{V}_j \quad \mathbf{U}_j] = \mathbf{I}, \mathbf{U}_j^T \mathbf{H}_f^j = \mathbf{0} \\ &= \|\tilde{\mathbf{x}}_k\|_{\mathbf{P}_{k|k-1}}^2 + \|\tilde{\mathbf{z}}_{k-N:k} - \mathbf{H}_x \tilde{\mathbf{x}}_{k-N:k}\|^2 \end{aligned}$$



Frontend: Multi-state Constraint Kalman Filter (MSCKF) [1]

- Step 3: Update $[O(M^3)]$

$$\begin{aligned} C'_{k|k} &= \|\tilde{\mathbf{x}}_k\|_{\mathbf{P}_{k|k-1}}^2 + \|\tilde{\mathbf{z}}_{k-N:k} - \mathbf{H}_x \tilde{\mathbf{x}}_{k-N:k}\|^2 \\ &= \|\tilde{\mathbf{x}}_{k-N:k}\|_{\mathbf{P}_{k-N:k}^\oplus}^2 \end{aligned}$$



Frontend: Multi-state Constraint Kalman Filter (MSCKF) [1]

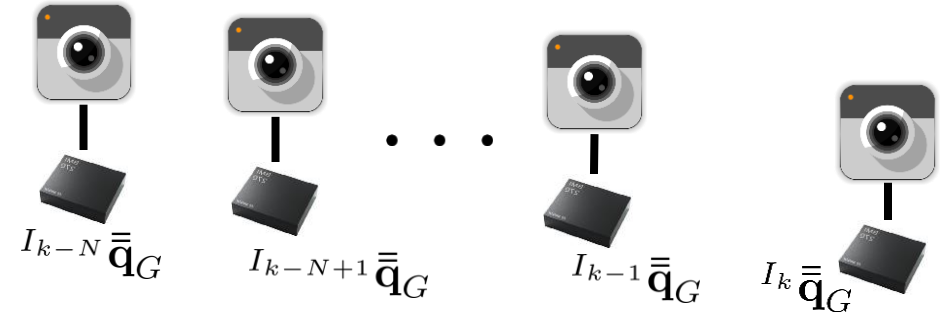
- Step 3: Update $[O(M^3)]$

$$\begin{aligned} \mathcal{C}'_{k|k} &= \|\tilde{\mathbf{x}}_k\|_{\mathbf{P}_{k|k-1}}^2 + \|\tilde{\mathbf{z}}_{k-N:k} - \mathbf{H}_x \tilde{\mathbf{x}}_{k-N:k}\|^2 \\ &= \|\tilde{\mathbf{x}}_{k-N:k}\|_{\mathbf{P}_{k-N:k}^\oplus}^2 \end{aligned}$$

- Step 4: Marginalize the oldest pose $I_{k-N} \bar{\mathbf{q}}_G$

$$\mathcal{C}'_{k|k} = \|\tilde{\mathbf{x}}_{k-N:k}\|_{\mathbf{P}_{k-N:k}^\oplus}^2$$

$$\mathcal{C}'_{k|k} = \|\tilde{\mathbf{x}}_{k-N+1:k}\|_{\mathbf{P}_{k-N+1:k}^\oplus}^2 + \|\mathbf{L}_1 I_{k-N} \tilde{\tilde{\mathbf{q}}}_G + \mathbf{L}_2 \tilde{\mathbf{x}}_{k-N+1:k}\|^2$$



Frontend: Multi-state Constraint Kalman Filter (MSCKF) [1]

- Step 3: Update $[O(M^3)]$

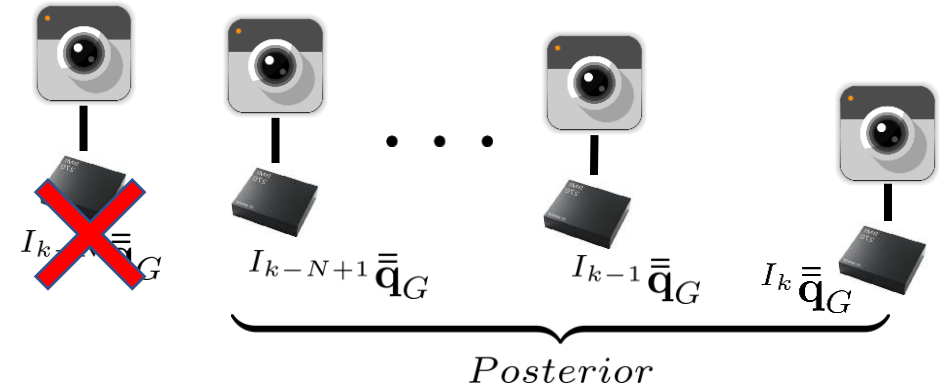
$$\begin{aligned} \mathcal{C}'_{k|k} &= \|\tilde{\mathbf{x}}_k\|_{\mathbf{P}_{k|k-1}}^2 + \|\tilde{\mathbf{z}}_{k-N:k} - \mathbf{H}_x \tilde{\mathbf{x}}_{k-N:k}\|^2 \\ &= \|\tilde{\mathbf{x}}_{k-N:k}\|_{\mathbf{P}_{k-N:k}^\oplus}^2 \end{aligned}$$

- Step 4: Marginalize the oldest pose $I_{k-N} \bar{\mathbf{q}}_G$

$$\mathcal{C}'_{k|k} = \|\tilde{\mathbf{x}}_{k-N:k}\|_{\mathbf{P}_{k-N:k}^\oplus}^2$$

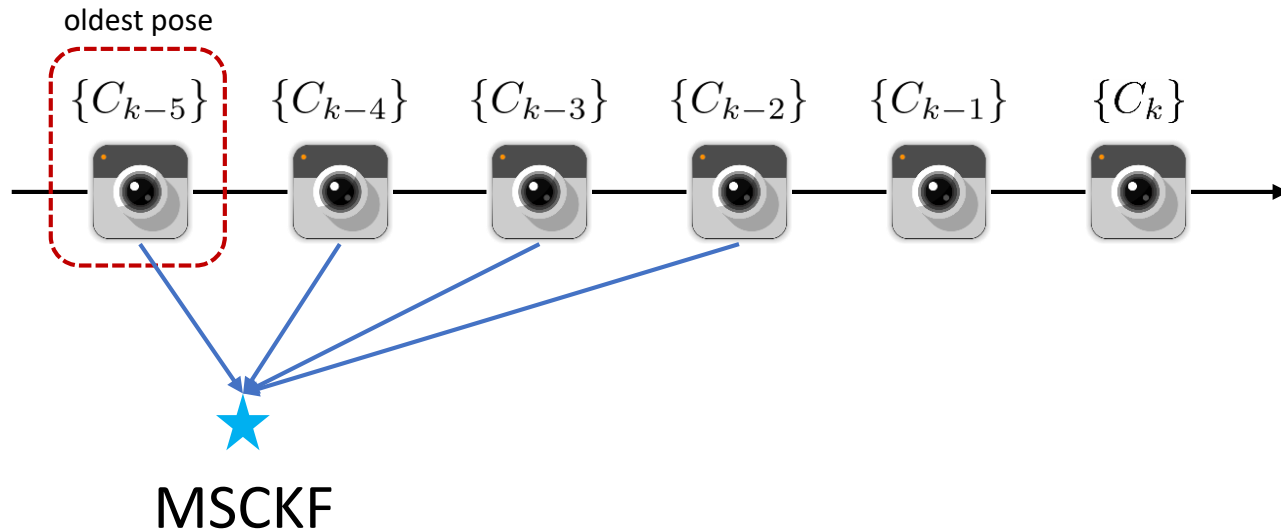
$$\mathcal{C}'_{k|k} = \|\tilde{\mathbf{x}}_{k-N+1:k}\|_{\mathbf{P}_{k-N+1:k}^\oplus}^2 + \|\mathbf{L}_1 I_{k-N} \tilde{\mathbf{q}}_G + \mathbf{L}_2 \tilde{\mathbf{x}}_{k-N+1:k}\|^2$$

$$\mathcal{C}''_{k|k} = \underbrace{\|\tilde{\mathbf{x}}_{k-N+1:k}\|_{\mathbf{P}_{k-N+1:k}^\oplus}^2}_{\text{Posterior}}$$



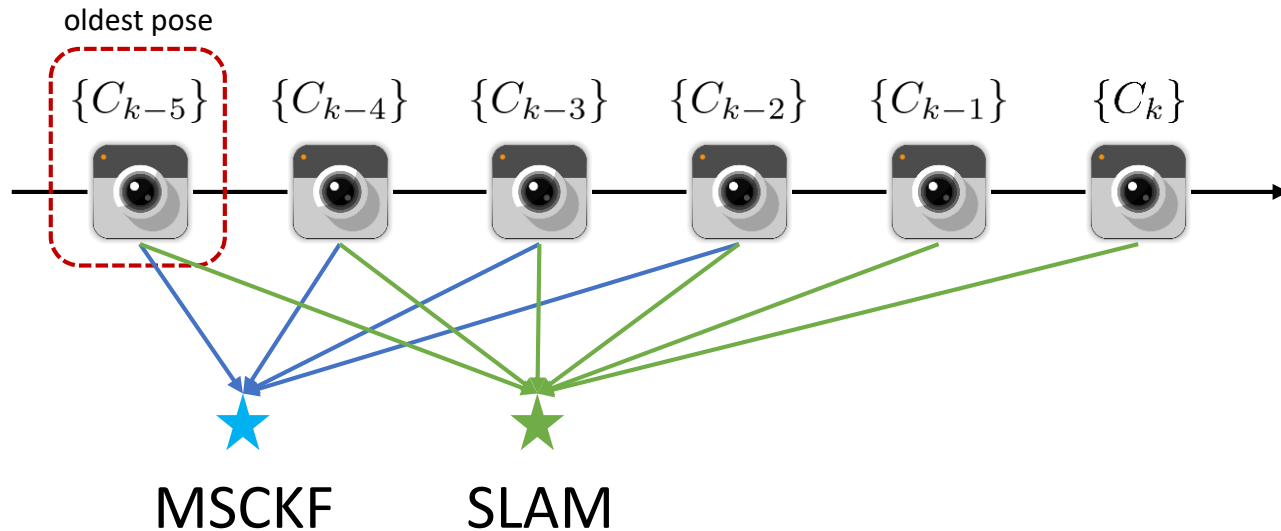
MSCKF Feature Classification & Processing

- Mature feature: Track starts at the oldest pose (to be marginalized)
 - Track spans part of the window -> Marginalize w/ **MSCKF**



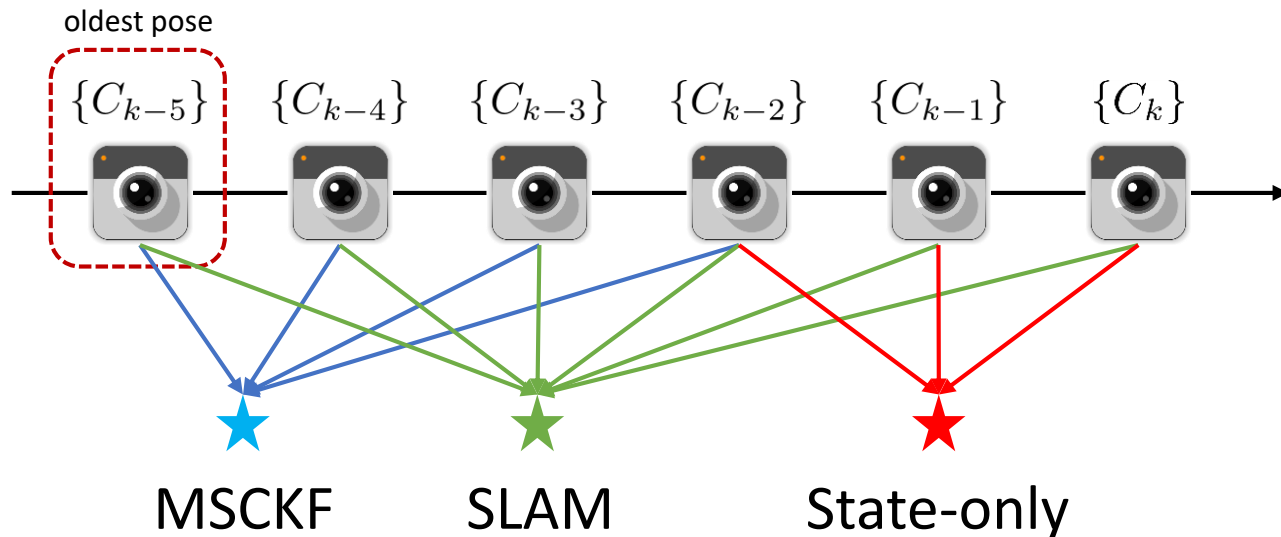
MSCKF Feature Classification & Processing

- Mature feature: Track starts at the oldest pose (to be marginalized)
 - Track spans part of the window -> Marginalize w/ **MSCKF**
 - Track spans the whole window -> Add to the state vector as **SLAM** feature



MSCKF Feature Classification & Processing

- Mature feature: Track starts at the oldest pose (to be marginalized)
 - Track spans part of the window -> Marginalize w/ **MSCKF**
 - Track spans the whole window -> Add to the state vector as **SLAM** feature
- Immature feature: Track is still ongoing
 - Use as **state-only** feature (update states, but not covariance)



Filtering vs. Optimization-based Methods

- MSCKF (EKF) \iff MAP estimator w/ one Gauss-Newton iteration ^[1]
 - Iteratively processes camera meas/nts (Iterated EKF ^[2]), IMU meas/nts (IKS ^[3])
- MSCKF (EKF) \iff SWF (EIF) ^[4]
- Square-root variants: SR-EKF, SR-EIF ^[5]
 - Use Cholesky factor of covariance/Hessian
 - Better numerical properties
 - Single-precision arithmetic (4x speed up for ARM Neon coprocessor)

	EKF	EIF
Prior	Covariance \mathbf{P}	Information \mathbf{A}
Propagation	$\mathbf{P} \leftarrow \begin{bmatrix} \mathbf{P} & \mathbf{P}\Phi^T \\ \Phi\mathbf{P} & \Phi\mathbf{P}\Phi^T + \mathbf{W} \end{bmatrix}$	$\mathbf{A} \leftarrow \begin{bmatrix} \mathbf{A} + \Phi^T \mathbf{W}^{-1} \Phi & -\Phi^T \mathbf{W}^{-1} \\ -\mathbf{W}^{-1} \Phi & \mathbf{W}^{-1} \end{bmatrix}$
Update	$\mathbf{S} = \mathbf{H}\mathbf{P}\mathbf{H}^T + \Sigma$ $\mathbf{P}^\oplus = \mathbf{P} - \mathbf{P}\mathbf{H}^T \mathbf{S}^{-1} \mathbf{H}\mathbf{P}$ $\mathbf{P} \leftarrow \mathbf{P}^\oplus$ $\Delta \mathbf{x} = \mathbf{P}\mathbf{H}^T \mathbf{S}^{-1} \mathbf{r}$	$\mathbf{A}^\oplus = \mathbf{A} + \mathbf{H}^T \Sigma^{-1} \mathbf{H}$ $\mathbf{b}^\oplus = \mathbf{H}^T \Sigma^{-1} \mathbf{r}$ $\mathbf{A} \leftarrow \mathbf{A}^\oplus$ $\Delta \mathbf{x} = \mathbf{A}^{\oplus -1} \mathbf{b}^\oplus$
Marginalization	$\mathbf{P}\mathbf{P}\mathbf{P}^T = \begin{bmatrix} \mathbf{P}_{\mu\mu} & \mathbf{P}_{\mu\rho} \\ \mathbf{P}_{\rho\mu} & \mathbf{P}_{\rho\rho} \end{bmatrix}$ $\mathbf{P} \leftarrow \mathbf{P}_{\rho\rho}$	$\mathbf{A}\mathbf{A}\mathbf{A}^T = \begin{bmatrix} \mathbf{A}_{\mu\mu} & \mathbf{A}_{\mu\rho} \\ \mathbf{A}_{\rho\mu} & \mathbf{A}_{\rho\rho} \end{bmatrix}$ $\mathbf{A}'_{\rho\rho} = \mathbf{A}_{\rho\rho} - \mathbf{A}_{\rho\mu} \mathbf{A}_{\mu\mu}^{-1} \mathbf{A}_{\mu\rho}$ $\mathbf{A} \leftarrow \mathbf{A}'_{\rho\rho}$

[1] A. H. Jazwinski, **Stochastic processes and filtering theory**, Academic Press, 1970

[2] P. S. Maybeck, **Stochastic Models, Estimation and Control**, vol. 1, Academic Press, 1979

[3] D. G. Kottas and S. I. Roumeliotis, "An iterative Kalman smoother for robust 3D localization on mobile and wearable devices," ICRA'15

[4] G. Sibley, L. Matthies, and G. Sukhatme, "Sliding window filter with application to planetary landing," JFR'10

[5] K. J. Wu, A. Ahmed, G. Georgiou, and S. I. Roumeliotis, "A square root inverse filter for efficient vision-aided inertial navigation on mobile devices," RSS'15

Inconsistency of VIO

Due to mismatch of observability properties btwn nonlinear system and linearized estimator [1,2,3,4]

[1] S. Julier and J. Uhlmann, “A counter example to the theory of simultaneous localization and map building,” ICRA’01

[2] J. A. Castellanos, J. Neira, and J. D. Tardos, “Limits to the consistency of EKF-based slam,” IFAC’04

[3] G. P. Huang, A. I. Mourikis, and S. I. Roumeliotis, “Observability-based rules for designing consistent EKF SLAM estimators,” IJRR’10

[4] J. A. Hesch, D. G. Kottas, S. L. Bowman, and S. I. Roumeliotis, “Camera-IMU-based localization: Observability analysis and consistency improvement,” IJRR’14

Inconsistency of VIO

Due to mismatch of observability properties btwn nonlinear system and linearized estimator [1,2,3,4]

Actual nonlinear system

$$\begin{cases} \dot{\mathbf{x}} &= \mathbf{f}_0(\mathbf{x}) + \sum_{i=1}^l \mathbf{f}_i(\mathbf{u}) \\ \mathbf{z} &= \mathbf{h}(\mathbf{x}) \end{cases}$$

- Inf. dim.
- Full col. rank
- Observable

$$\mathcal{O} = \begin{bmatrix} \nabla \mathcal{L}^0 \mathbf{h} \\ \nabla \mathcal{L}_{\mathbf{f}_i}^1 \mathbf{h} \\ \nabla \mathcal{L}_{\mathbf{f}_i \mathbf{f}_j}^2 \mathbf{h} \\ \nabla \mathcal{L}_{\mathbf{f}_i \mathbf{f}_j \mathbf{f}_k}^3 \mathbf{h} \\ \vdots \end{bmatrix}$$

$$= \begin{bmatrix} \frac{\partial \mathcal{L}^0 \mathbf{h}}{\partial \beta} \\ \frac{\partial \mathcal{L}_{\mathbf{f}_i}^1 \mathbf{h}}{\partial \beta} \\ \frac{\partial \mathcal{L}_{\mathbf{f}_i \mathbf{f}_j}^2 \mathbf{h}}{\partial \beta} \\ \frac{\partial \mathcal{L}_{\mathbf{f}_i \mathbf{f}_j \mathbf{f}_k}^3 \mathbf{h}}{\partial \beta} \\ \vdots \end{bmatrix}$$

$$\frac{\partial \beta}{\partial \mathbf{x}} = \begin{bmatrix} \mathbf{E} & \mathbf{B} \end{bmatrix}$$

- Finite. dim.
- Null(O) = Null(B)

Global trans.

$$\text{Null}(\mathcal{O})_{VIO} = \begin{bmatrix} \mathbf{0}_3 & I_G \mathbf{C}^G \mathbf{g} \\ \mathbf{0}_3 & \mathbf{0}_3 \\ \mathbf{0}_3 & -[\mathbf{v} \times]^G \mathbf{g} \\ \mathbf{0}_3 & \mathbf{0}_3 \\ \mathbf{I}_3 & -[\mathbf{p} \times]^G \mathbf{g} \\ \mathbf{I}_3 & -[\mathbf{p}_f \times]^G \mathbf{g} \end{bmatrix} \begin{bmatrix} \theta \\ \mathbf{b}_g \\ \mathbf{v} \\ \mathbf{b}_a \\ \mathbf{p} \\ \mathbf{p}_f \end{bmatrix} = \begin{bmatrix} \mathbf{N}_t & | & \mathbf{N}_r \end{bmatrix}$$

Rot. around gravity

Ideal linearized system

$$\begin{cases} \mathbf{x}_{k+1|k} &= \Phi_{k|k} \mathbf{x}_{k|k} + \mathbf{G}_{k|k} \mathbf{u}_k \\ \mathbf{z}_k &= \mathbf{H}_{k|k} \hat{\mathbf{x}}_{k|k} \end{cases}$$

[3] G. P. Huang, A. I. Mourikis, and S. I. Roumeliotis, "Observability-based rules for designing consistent EKF SLAM estimators," *IJRR'10*

[4] J. A. Hesck, D. G. Kottas, S. L. Bowman, and S. I. Roumeliotis, "Camera-IMU-based localization: Observability analysis and consistency improvement," *IJRR'14*

Inconsistency of VIO

Due to mismatch of observability properties btwn nonlinear system and linearized estimator [1,2,3,4]

Actual nonlinear system

$$\begin{cases} \dot{\mathbf{x}} = \mathbf{f}_0(\mathbf{x}) + \sum_{i=1}^l \mathbf{f}_i(\mathbf{u}) \\ \mathbf{z} = \mathbf{h}(\mathbf{x}) \end{cases}$$

- Inf. dim.
- Full col. rank
- Observable

$$\mathcal{O} = \begin{bmatrix} \nabla \mathcal{L}^0 \mathbf{h} \\ \nabla \mathcal{L}_{\mathbf{f}_i}^1 \mathbf{h} \\ \nabla \mathcal{L}_{\mathbf{f}_i \mathbf{f}_j}^2 \mathbf{h} \\ \nabla \mathcal{L}_{\mathbf{f}_i \mathbf{f}_j \mathbf{f}_k}^3 \mathbf{h} \\ \vdots \end{bmatrix} = \begin{bmatrix} \frac{\partial \mathcal{L}^0 \mathbf{h}}{\partial \beta} \\ \frac{\partial \mathcal{L}_{\mathbf{f}_i}^1 \mathbf{h}}{\partial \beta} \\ \frac{\partial \mathcal{L}_{\mathbf{f}_i \mathbf{f}_j}^2 \mathbf{h}}{\partial \beta} \\ \frac{\partial \mathcal{L}_{\mathbf{f}_i \mathbf{f}_j \mathbf{f}_k}^3 \mathbf{h}}{\partial \beta} \\ \vdots \end{bmatrix}$$

$$\frac{\partial \beta}{\partial \mathbf{x}} = \begin{bmatrix} \mathbf{E} & \mathbf{B} \end{bmatrix}$$

- Finite. dim.
- Null(O) = Null(B)

Global trans.

$$\text{Null}(\mathcal{O})_{VIO} = \begin{bmatrix} \mathbf{0}_3 & \mathbf{I}_G \mathbf{C}^G \mathbf{g} \\ \mathbf{0}_3 & \mathbf{0}_3 \\ \mathbf{0}_3 & -[\mathbf{v} \times]^G \mathbf{g} \\ \mathbf{0}_3 & \mathbf{0}_3 \\ \mathbf{I}_3 & -[\mathbf{p} \times]^G \mathbf{g} \\ \mathbf{I}_3 & -[\mathbf{p}_f \times]^G \mathbf{g} \end{bmatrix} \begin{bmatrix} \theta \\ \mathbf{b}_g \\ \mathbf{v} \\ \mathbf{b}_a \\ \mathbf{p} \\ \mathbf{p}_f \end{bmatrix} = \begin{bmatrix} \mathbf{N}_t & | & \mathbf{N}_r \end{bmatrix}$$

Rot. around gravity

Ideal linearized system

$$\begin{cases} \mathbf{x}_{k+1|k} = \Phi_{k|k} \mathbf{x}_{k|k} + \mathbf{G}_{k|k} \mathbf{u}_k \\ \mathbf{z}_k = \mathbf{H}_{k|k} \hat{\mathbf{x}}_{k|k} \end{cases}$$

$$\mathbf{M} = \begin{bmatrix} & & \mathbf{H}_k & & \\ & & \mathbf{H}_{k+1} \Phi_{k|k} & & \\ & & \vdots & & \\ \mathbf{H}_{k+m} \Phi_{k+m-1|k+m-1} & \cdots & \Phi_{k|k} & & \end{bmatrix}$$

Actual linearized estimator

$$\begin{cases} \hat{\mathbf{x}}_{k+1|k} = \hat{\Phi}_{k|k} \hat{\mathbf{x}}_{k|k} + \hat{\mathbf{G}}_{k|k} \mathbf{u}_k \\ \mathbf{z}_k = \hat{\mathbf{H}}_{k|k} \hat{\mathbf{x}}_{k|k} \end{cases}$$

$$\hat{\mathbf{M}} = \begin{bmatrix} & & \hat{\mathbf{H}}_k & & \\ & & \hat{\mathbf{H}}_{k+1} \hat{\Phi}_{k|k} & & \\ & & \vdots & & \\ \hat{\mathbf{H}}_{k+m} \hat{\Phi}_{k+m-1|k+m-1} & \cdots & \hat{\Phi}_{k|k} & & \end{bmatrix}$$

$$\text{Null}(\mathbf{M}) = \text{Null}(\mathcal{O})_{VIO} \not\supseteq \text{Null}(\hat{\mathbf{M}}) = \mathbf{N}_t$$

[3] G. P. Huang, A. I. Mourikis, and S. I. Roumeliotis, "Observability-based rules for designing consistent EKF SLAM estimators," *IJRR'10*

[4] J. A. Hesck, D. G. Kottas, S. L. Bowman, and S. I. Roumeliotis, "Camera-IMU-based localization: Observability analysis and consistency improvement," *IJRR'14*

Inconsistency of VIO

Due to mismatch of observability properties btwn nonlinear system and linearized estimator [1,2,3,4]

Actual nonlinear system

$$\begin{cases} \dot{\mathbf{x}} = \mathbf{f}_0(\mathbf{x}) + \sum_{i=1}^l \mathbf{f}_i(\mathbf{u}) \\ \mathbf{z} = \mathbf{h}(\mathbf{x}) \end{cases}$$

- Inf. dim.
- Full col. rank
- Observable

$$\mathcal{O} = \begin{bmatrix} \nabla \mathcal{L}^0 \mathbf{h} \\ \nabla \mathcal{L}_{f_i}^1 \mathbf{h} \\ \nabla \mathcal{L}_{f_i f_j}^2 \mathbf{h} \\ \nabla \mathcal{L}_{f_i f_j f_k}^3 \mathbf{h} \\ \vdots \end{bmatrix} = \begin{bmatrix} \frac{\partial \mathcal{L}^0 \mathbf{h}}{\partial \beta} \\ \frac{\partial \mathcal{L}_{f_i}^1 \mathbf{h}}{\partial \beta} \\ \frac{\partial \mathcal{L}_{f_i f_j}^2 \mathbf{h}}{\partial \beta} \\ \frac{\partial \mathcal{L}_{f_i f_j f_k}^3 \mathbf{h}}{\partial \beta} \\ \vdots \end{bmatrix}$$

$$\frac{\partial \beta}{\partial \mathbf{x}} = \begin{bmatrix} \mathbf{E} & \mathbf{B} \end{bmatrix}$$

- Finite. dim.
- Null(O) = Null(B)

Global trans.

$$\text{Null}(\mathcal{O})_{VIO} = \begin{bmatrix} \mathbf{0}_3 & I_G \mathbf{C}^G \mathbf{g} \\ \mathbf{0}_3 & \mathbf{0}_3 \\ \mathbf{0}_3 & -[\mathbf{v} \times]^G \mathbf{g} \\ \mathbf{0}_3 & \mathbf{0}_3 \\ \mathbf{I}_3 & -[\mathbf{p} \times]^G \mathbf{g} \\ \mathbf{I}_3 & -[\mathbf{p}_f \times]^G \mathbf{g} \end{bmatrix} \begin{bmatrix} \theta \\ \mathbf{b}_g \\ \mathbf{v} \\ \mathbf{b}_a \\ \mathbf{p} \\ \mathbf{p}_f \end{bmatrix} = \begin{bmatrix} \mathbf{N}_t & | & \mathbf{N}_r \end{bmatrix}$$

Rot. around gravity

Ideal linearized system

$$\begin{cases} \mathbf{x}_{k+1|k} = \Phi_{k|k} \mathbf{x}_{k|k} + \mathbf{G}_{k|k} \mathbf{u}_k \\ \mathbf{z}_k = \mathbf{H}_{k|k} \hat{\mathbf{x}}_{k|k} \end{cases}$$

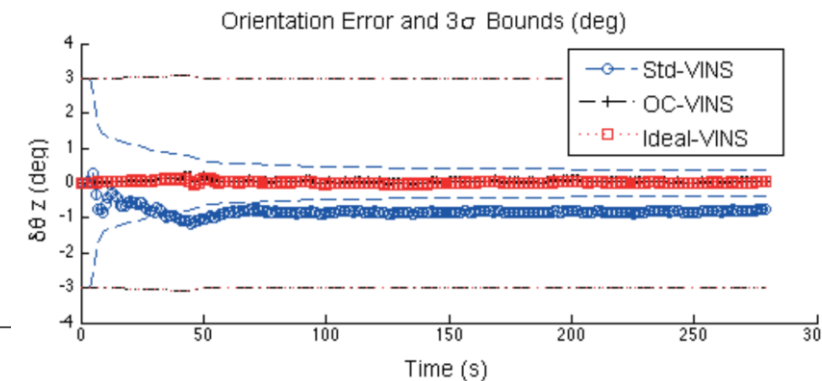
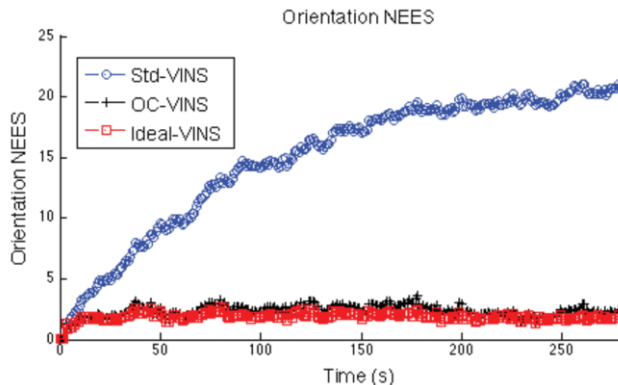
$$\mathbf{M} = \begin{bmatrix} \mathbf{H}_k & & & \\ & \mathbf{H}_{k+1} \Phi_{k|k} & & \\ & & \ddots & \\ \mathbf{H}_{k+m} \Phi_{k+m-1|k+m-1} & \cdots & \Phi_{k|k} & \end{bmatrix}$$

Actual linearized estimator

$$\begin{cases} \hat{\mathbf{x}}_{k+1|k} = \hat{\Phi}_{k|k} \hat{\mathbf{x}}_{k|k} + \hat{\mathbf{G}}_{k|k} \mathbf{u}_k \\ \mathbf{z}_k = \hat{\mathbf{H}}_{k|k} \hat{\mathbf{x}}_{k|k} \end{cases}$$

$$\hat{\mathbf{M}} = \begin{bmatrix} & & & \hat{\mathbf{H}}_k \\ & & & \hat{\mathbf{H}}_{k+1} \hat{\Phi}_{k|k} \\ & & \ddots & \\ \hat{\mathbf{H}}_{k+m} \hat{\Phi}_{k+m-1|k+m-1} & \cdots & \hat{\Phi}_{k|k} & \end{bmatrix}$$

$$\text{Null}(\mathbf{M}) = \text{Null}(\mathcal{O})_{VIO} \not\supseteq \text{Null}(\hat{\mathbf{M}}) = \mathbf{N}_t$$

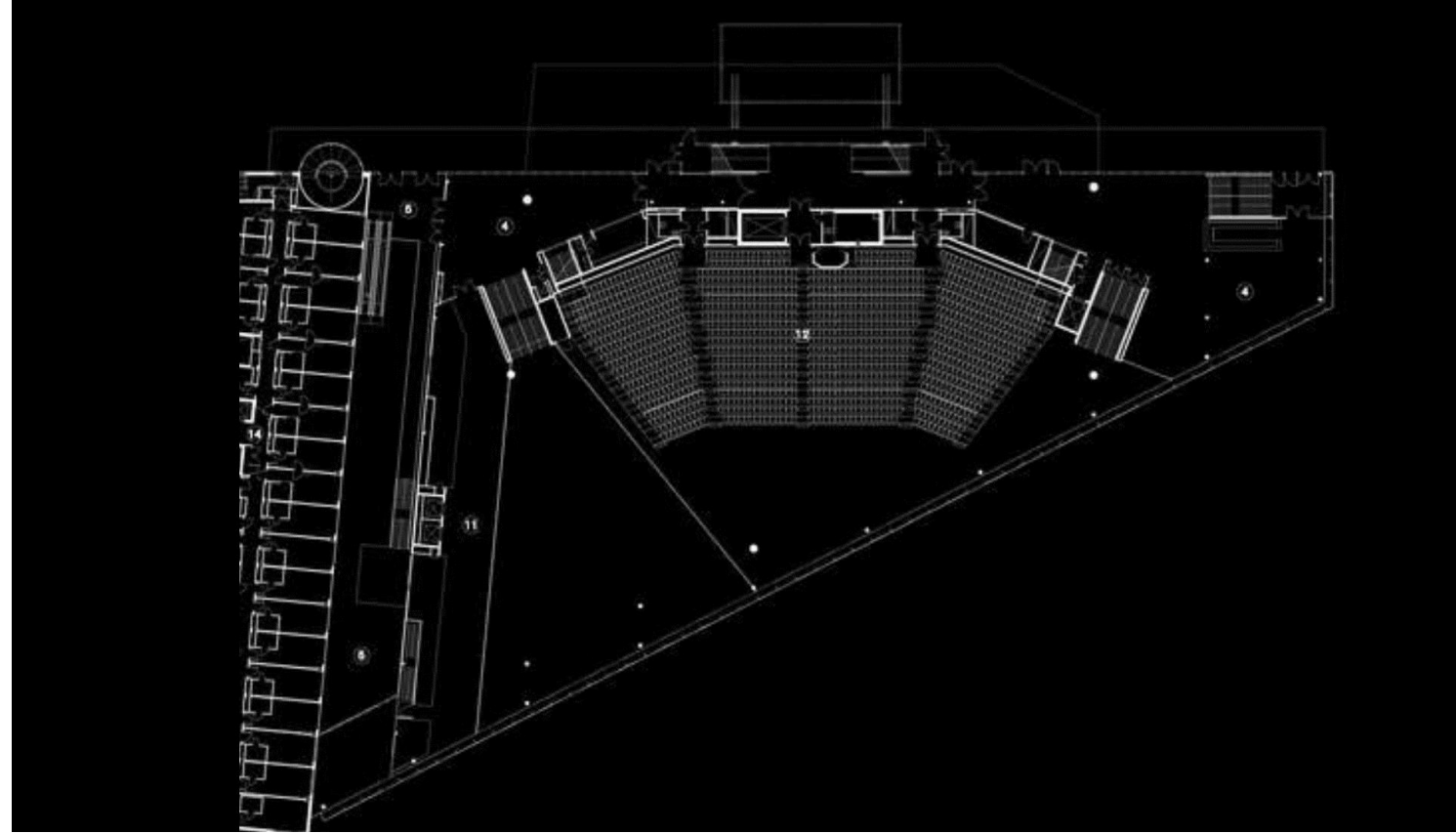


[3] G. P. Huang, A. I. Mourikis, and S. I. Roumeliotis, "Observability-based rules for designing consistent EKF SLAM estimators," *IJRR'10*

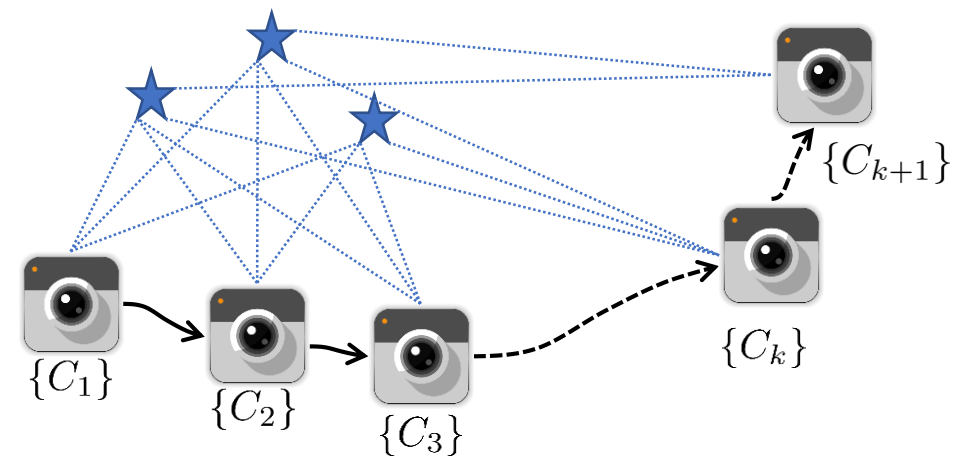
[4] J. A. Hesck, D. G. Kottas, S. L. Bowman, and S. I. Roumeliotis, "Camera-IMU-based localization: Observability analysis and consistency improvement," *IJRR'14*

Mapping Backend

- Offline: BA [1,2], CM [3]



ICRA'16



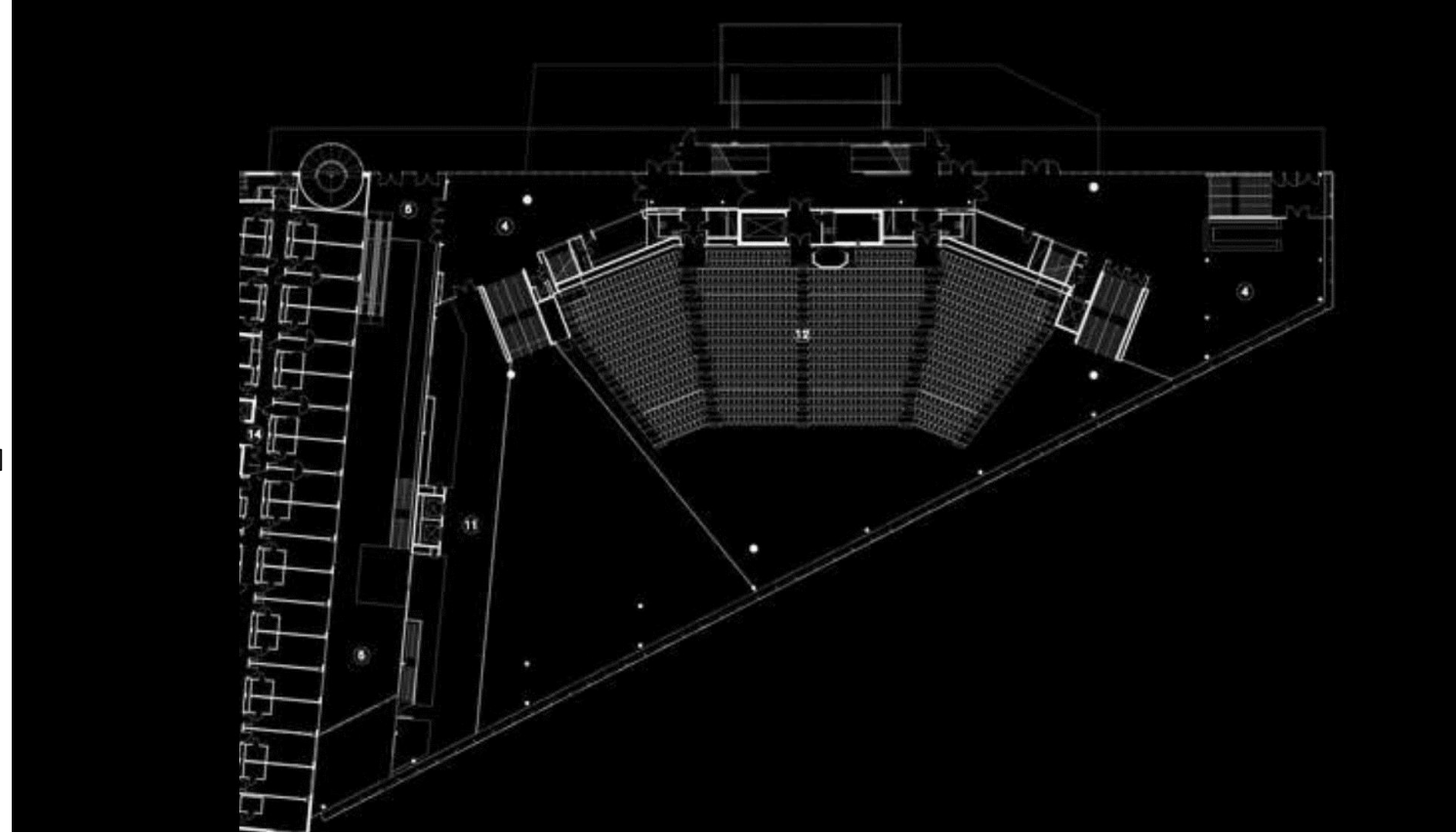
[1] B. Triggs, P. McLauchlan, R. Hartley, and A. Fitzgibbon, "Bundle Adjustment - A Modern Synthesis," Vision Algorithms: Theory and Practice, 2000

[2] S. Lynen, T. Sattler, M. Bosse, J. Hesch, M. Pollefeys, R. Siegwart, "Get Out of My Lab: Large-scale, Real-Time Visual-Inertial Localization," RSS'14

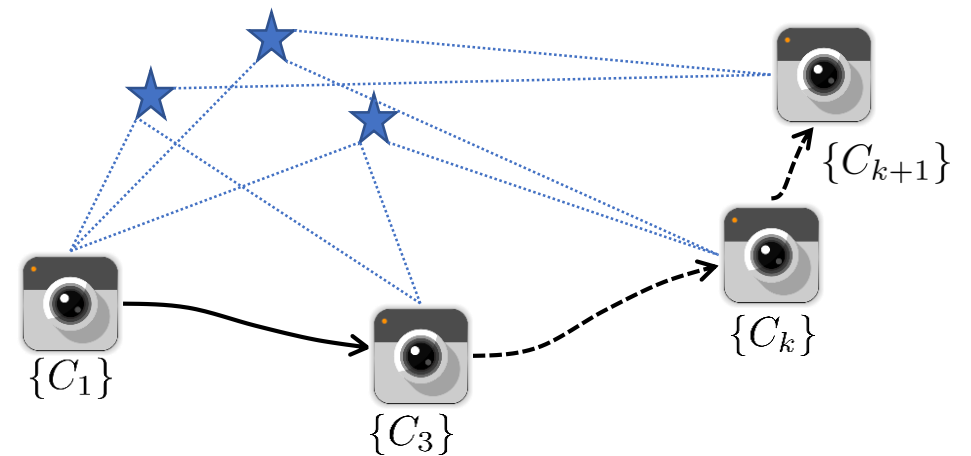
[3] C. Guo, K. Sartipi, R. DuToit, G. Georgiou, R. Li, J. O'Leary, E. Nerurkar, J. Hesch, and S. Roumeliotis, "Resource-Aware Large-Scale Cooperative Three-Dimensional Mapping Using Multiple Mobile Devices," TRO'18

Mapping Backend

- Offline: BA [1,2], CM [3]
- Online
 - BLS Approximation: PTAM[4], iSAM2[5], C-KLAM[6]
 - Employ approximations e.g., perfect keyframe/feature assumption, delay relinearization, duplicate meas/nts



ICRA'16



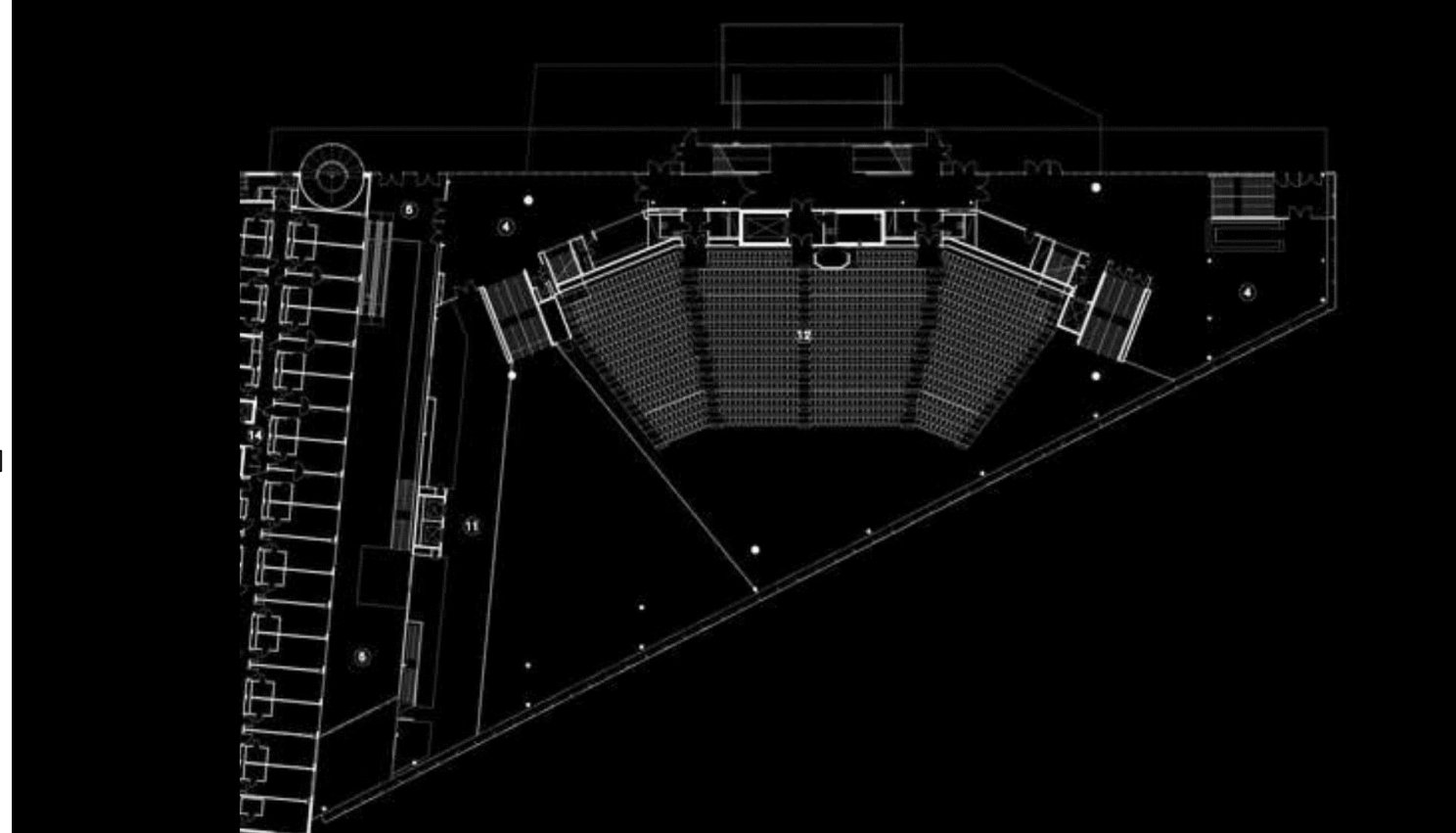
[4] G. Klein and D. Murray, "Parallel Tracking and Mapping for Small AR Workspaces," ISMAR'07

[5] M. Kaess, H. Johannsson, R. Roberts, V. Ila, J. Leonard, and F. Dellaert, "iSAM2: Incremental Smoothing and Mapping using the Bayes Tree," IJRR'12

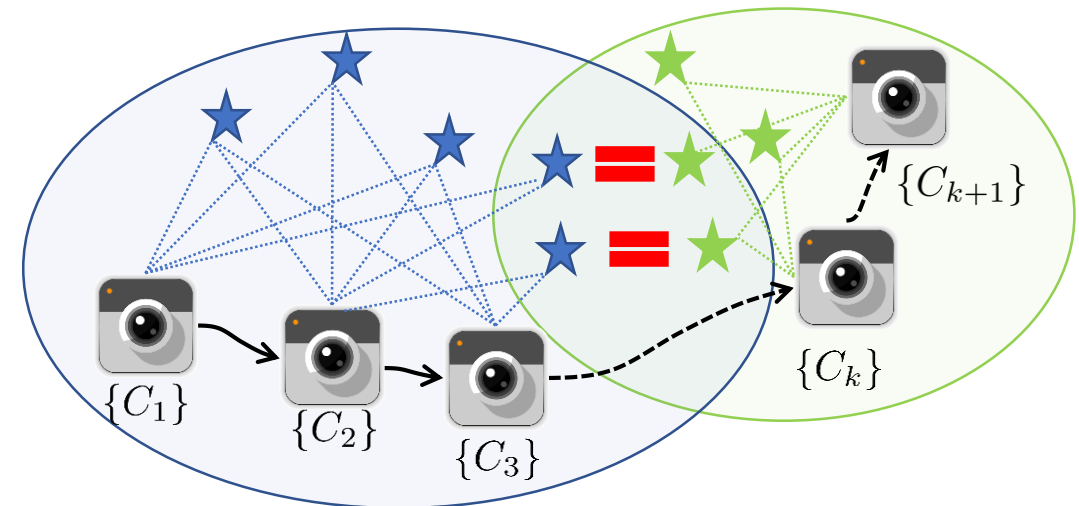
[6] E.D. Nerurkar, K.J. Wu, and S.I. Roumeliotis, "C-KLAM: Constrained Keyframe-Based Localization and Mapping," ICRA'14

Mapping Backend

- Offline: BA [1,2], CM [3]
- Online
 - BLS Approximation: PTAM[4], iSAM2[5], C-KLAM[6]
 - Employ approximations e.g., perfect keyframe/feature assumption, delay relinearization, duplicate meas/nts
 - Sub-mapping: Tectonic SAM [7], Gravity aligned sub-maps[8]
 - Divide map into submaps and merge



ICRA'16

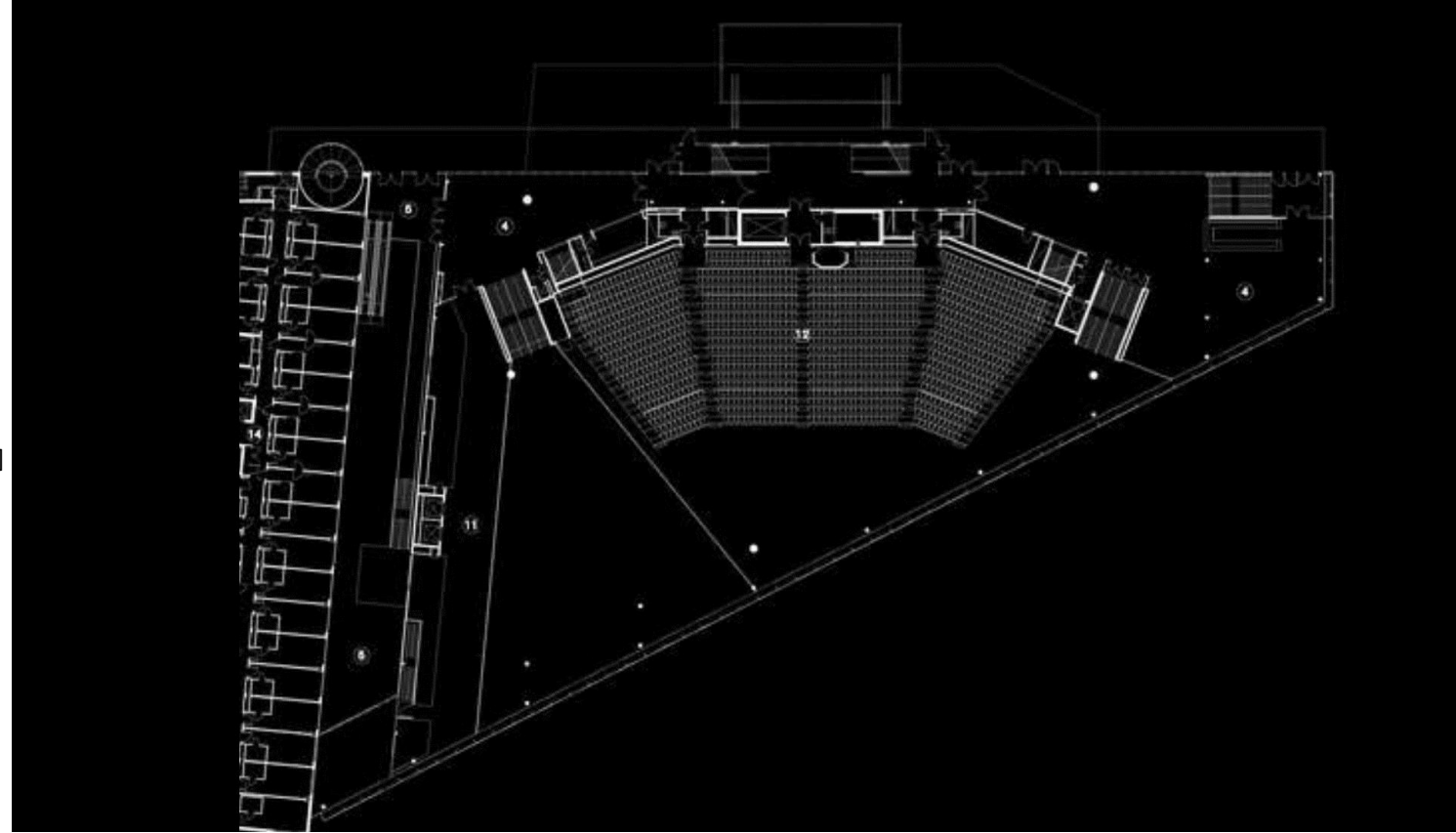


[7] K. Ni, D. Steedly, and F. Dellaert, "Tectonic SAM: Exact, out-of-core, submap-based SLAM," ICRA'07

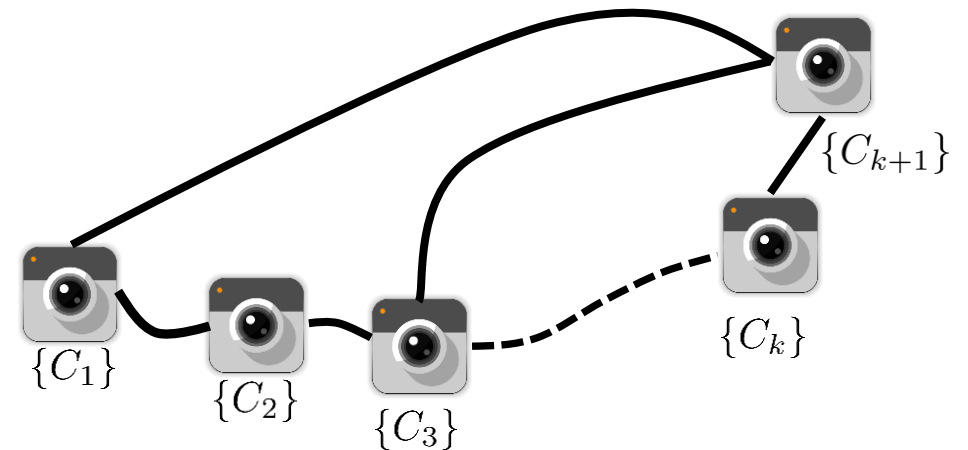
[8] K. Sartipi and S. Roumeliotis, "Efficient alignment of visual-inertial maps," ISER'18

Mapping Backend

- Offline: BA [1,2], CM [3]
- Online
 - BLS Approximation: PTAM[4], iSAM2[5], C-KLAM[6]
 - Employ approximations e.g., perfect keyframe/feature assumption, delay relinearization, duplicate meas/nts
 - Sub-mapping: Tectonic SAM [7], Gravity aligned sub-maps[8]
 - Divide map into submaps and merge
 - Pose-graph: Gutmann and Konolige [9], GraphSLAM[10], VINS-Mono [11]
 - Use features to determine relative poses and optimize only for poses



ICRA'16



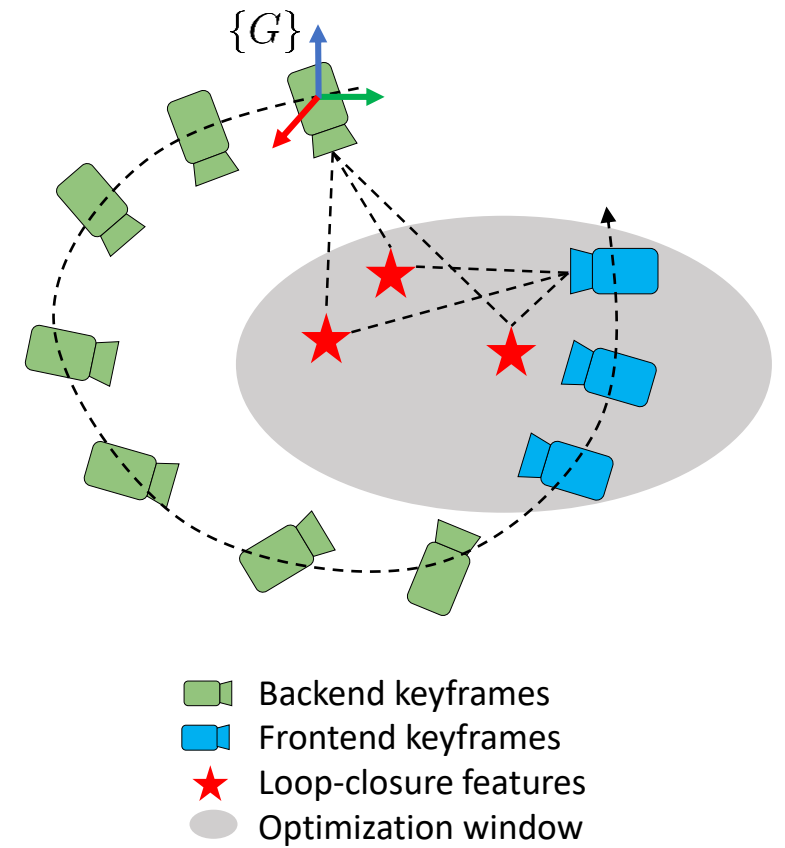
[9] J. Gutmann and K. Konolige, "Incremental Mapping of Large Cyclic Environments," CIRA'99

[10] S. Thrun and M. Montemerlo, "The GraphSLAM Algorithm with Applications to Large-Scale Mapping of Urban Structures," IJRR'05

[11] T. Qin, P. Li, and S. Shen, "VINS-Mono: A Robust and Versatile Monocular Visual-Inertial State Estimator," TRO'18

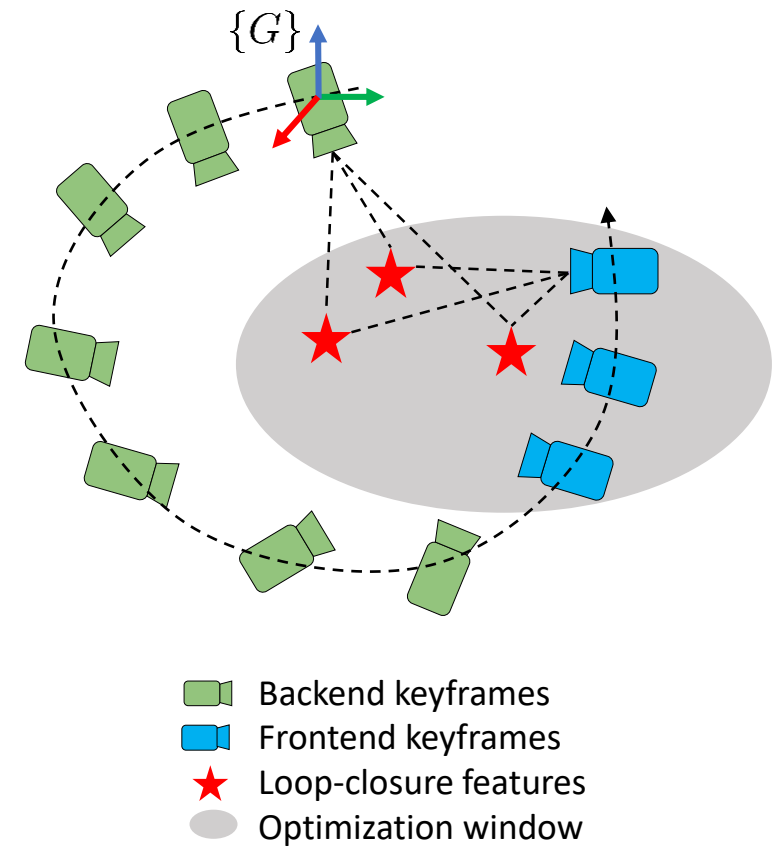
Map-based Updates

- Mapped keyframes/key features provided by the Backend to the Frontend



Map-based Updates

- Mapped keyframes/key features provided by the Backend to the Frontend
- Map assumed perfectly known^[1,2]



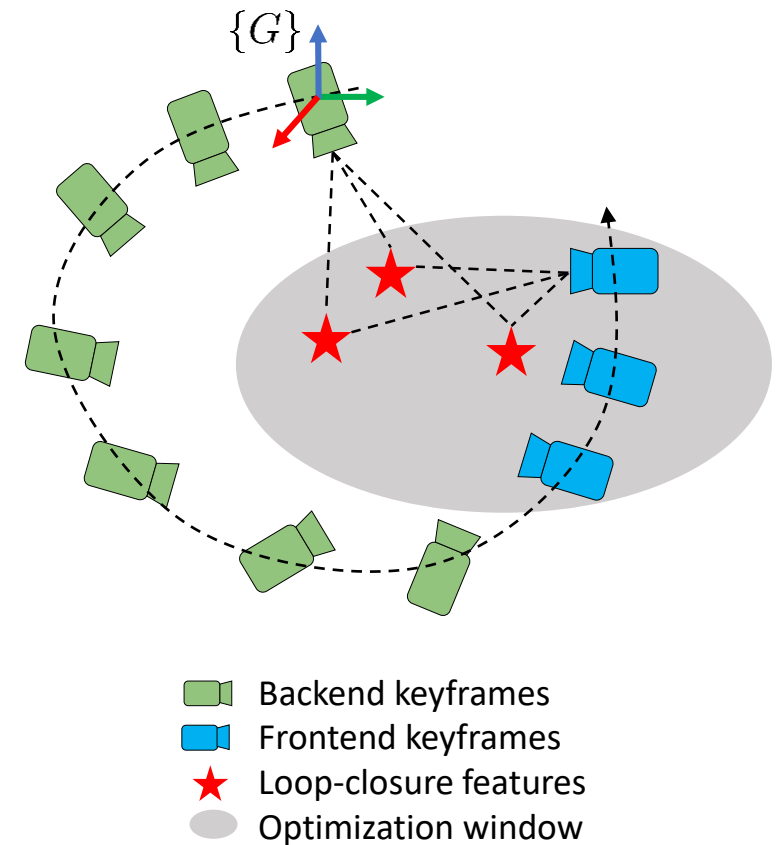
[1] A. Mourikis, N. Trawny, S. Roumeliotis, A. Johnson, A. Ansar, and L. Matthies, "Vision-Aided Inertial Navigation for Spacecraft Entry, Descent, and Landing," TRO'09

[2] S. Lynen, T. Sattler, M. Bosse, J. Hesch, M. Pollefeys, and R. Siegwart, "Get Out of My Lab: Large-scale, Real-Time Visual-Inertial Localization," RSS'14

Map-based Updates

- Mapped keyframes/key features provided by the Backend to the Frontend
- Map assumed perfectly known^[1,2]
 - Advantage: Constant processing cost
 - Disadvantage: Inconsistent

$$\mathcal{C}_{map} = \|\mathbf{z}_k^j - \mathbf{h}(\mathbf{x}_k, \mathbf{p}_{f_j})\|_{\sigma^2 \mathbf{I}}^2 \simeq \|\tilde{\mathbf{z}}_k^j - \mathbf{H}_k^j \tilde{\mathbf{x}}_k - \mathbf{H}_{f_j}^j \mathbf{p}_{f_j}\|_{\sigma^2 \mathbf{I}}^2$$



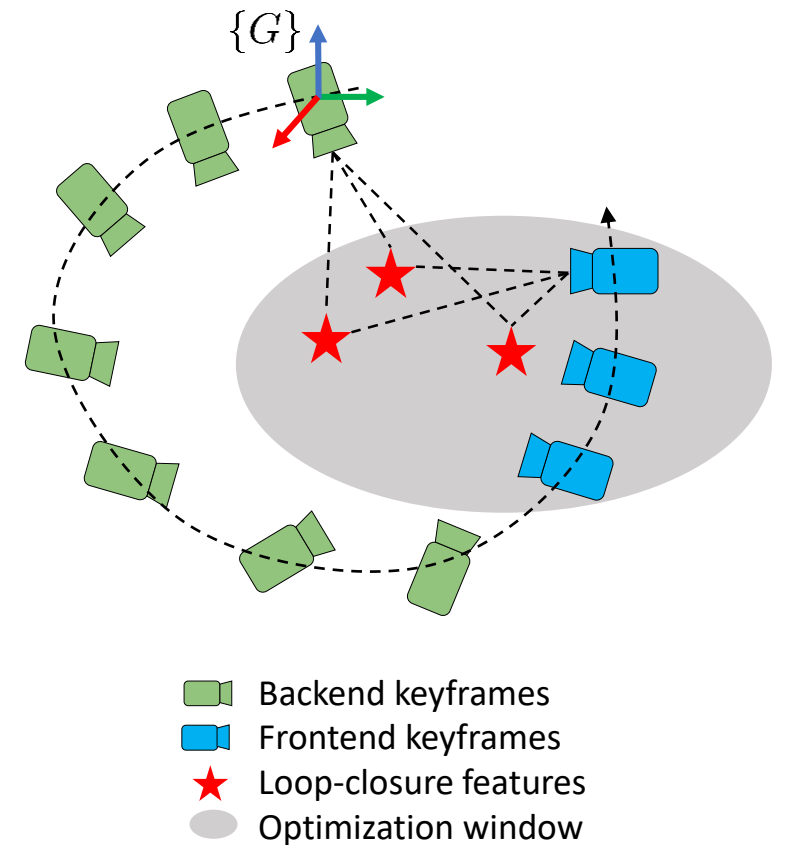
[1] A. Mourikis, N. Trawny, S. Roumeliotis, A. Johnson, A. Ansar, and L. Matthies, "Vision-Aided Inertial Navigation for Spacecraft Entry, Descent, and Landing," TRO'09

[2] S. Lynen, T. Sattler, M. Bosse, J. Hesch, M. Pollefeys, and R. Siegwart, "Get Out of My Lab: Large-scale, Real-Time Visual-Inertial Localization," RSS'14

Map-based Updates

- Mapped keyframes/key features provided by the Backend to the Frontend
- Map assumed perfectly known^[1,2]
 - Advantage: Constant processing cost
 - Disadvantage: Inconsistent
 - Remedy: Inflate meas/mnt noise

$$\mathcal{C}_{map} = \|\mathbf{z}_k^j - \mathbf{h}(\mathbf{x}_k, \mathbf{p}_{f_j})\|_{\sigma^2 \mathbf{I}}^2 \simeq \|\tilde{\mathbf{z}}_k^j - \mathbf{H}_k^j \tilde{\mathbf{x}}_k - \mathbf{H}_{f_j}^j \tilde{\mathbf{p}}_{f_j}\|_{4\sigma^2 \mathbf{I}}^2$$



[1] A. Mourikis, N. Trawny, S. Roumeliotis, A. Johnson, A. Ansar, and L. Matthies, "Vision-Aided Inertial Navigation for Spacecraft Entry, Descent, and Landing," TRO'09

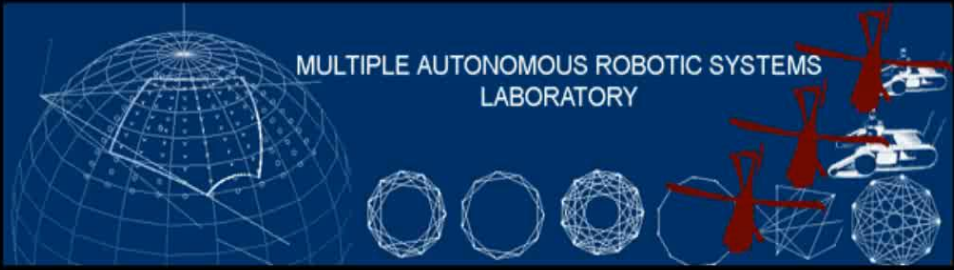
[2] S. Lynen, T. Sattler, M. Bosse, J. Hesch, M. Pollefeys, and R. Siegwart, "Get Out of My Lab: Large-scale, Real-Time Visual-Inertial Localization," RSS'14

Map-based Updates

- Mapped keyframes/key features provided by the Backend to the Frontend
- Map assumed perfectly known [1,2]
 - Advantage: Constant processing cost
 - Disadvantage: Inconsistent
 - Remedy: Inflate meas/mnt noise

$$C_{map} = \|\mathbf{z}_k^j - \mathbf{h}(\mathbf{x}_k, \mathbf{p}_{f_j})\|_{\sigma^2 \mathbf{I}}^2 \simeq \|\tilde{\mathbf{z}}_k^j - \mathbf{H}_k^j \tilde{\mathbf{x}}_k - \mathbf{H}_{f_j}^j \mathbf{p}_{f_j}\|_{4\sigma^2 \mathbf{I}}^2$$

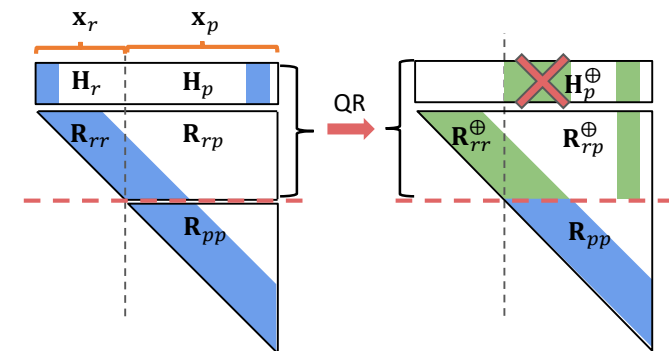
- Consistent alternatives:
 - Schmidt Kalman Filter [3]
 - RISE-SLAM [4]



MULTIPLE AUTONOMOUS ROBOTIC SYSTEMS
LABORATORY

A Vision-aided Inertial Navigation System with Map-based Corrections

MARS Lab
University of Minnesota
CVPR 2015



[1] A. Mourikis, N. Trawny, S. Roumeliotis, A. Johnson, A. Ansar, and L. Matthies, "Vision-Aided Inertial Navigation for Spacecraft Entry, Descent, and Landing," TRO'09

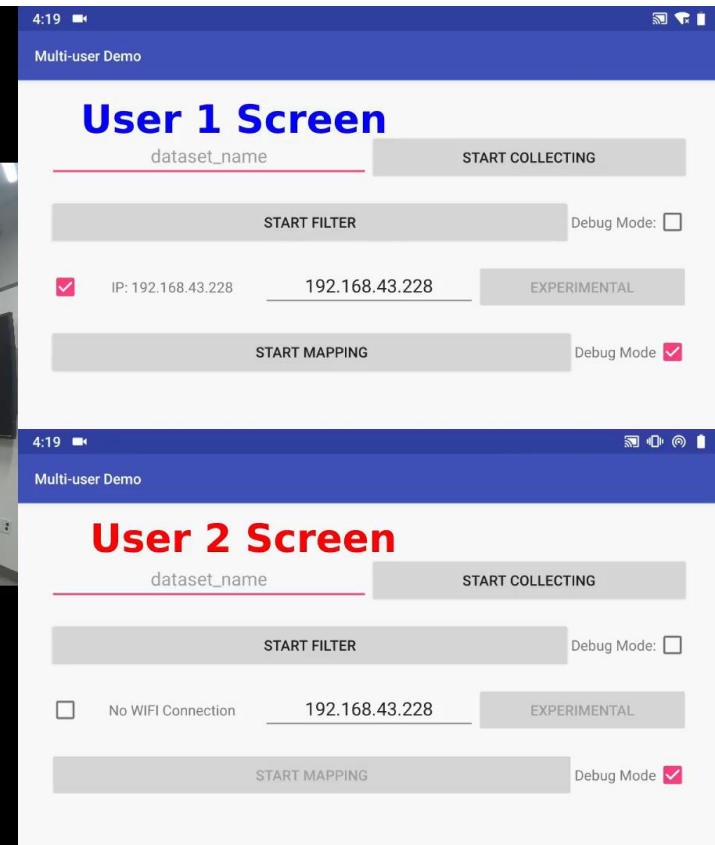
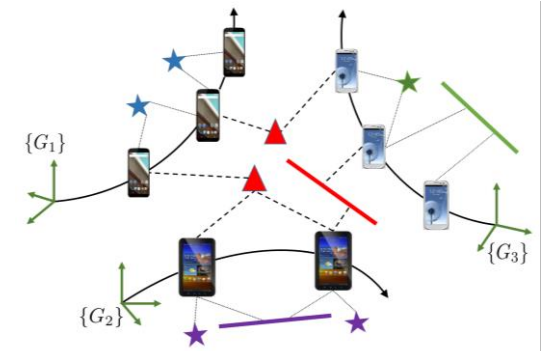
[2] S. Lynen, T. Sattler, M. Bosse, J. Hesch, M. Pollefeys, and R. Siegwart, "Get Out of My Lab: Large-scale, Real-Time Visual-Inertial Localization," RSS'14

[3] R. Dutoit, J. Hesch, E. Nerurkar, and S. Roumeliotis, "Consistent Map-based 3D Localization on Mobile Devices," ICRA'17

[4] T. Ke, K. Wu and S. Roumeliotis, "RISE-SLAM: A Resource-aware Inverse Schmidt Estimator for SLAM," IROS'19

Cooperative VIO/SLAM

- Data from multiple devices are fused to create an area representation
- Centralized [1,2]
 - Computation is offloaded from device
 - Require powerful server for processing

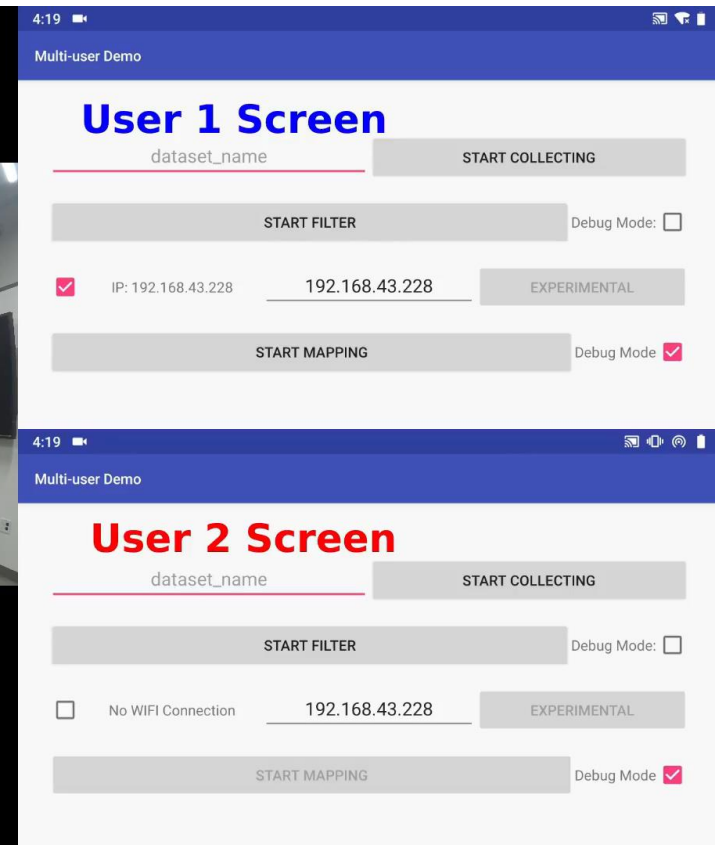
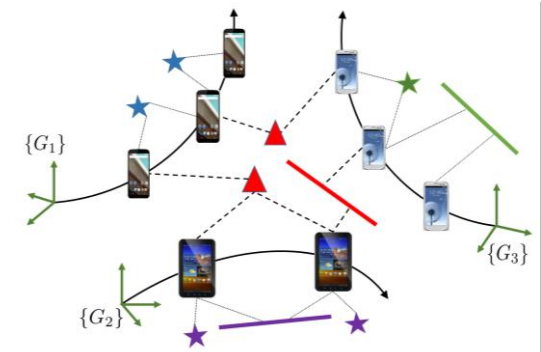


[1] M. Karrer, P. Schmuck, and M. Chli, "CVI-SLAM collaborative visual-inertial SLAM," RAL'18

[2] C. Guo, K. Sartipi, R. DuToit, G. Georgiou, R. Li, J. O'Leary, E. Nerurkar, J. Hesch, and S. Roumeliotis, "Resource-Aware Large-Scale Cooperative Three-Dimensional Mapping Using Multiple Mobile Devices," TRO'18

Cooperative VIO/SLAM

- Data from multiple devices are fused to create an area representation
- Centralized ^[1,2]
 - Computation is offloaded from device
 - Require powerful server for processing
- Distributed ^[3,4]
 - All devices cooperate to compute a single area representation

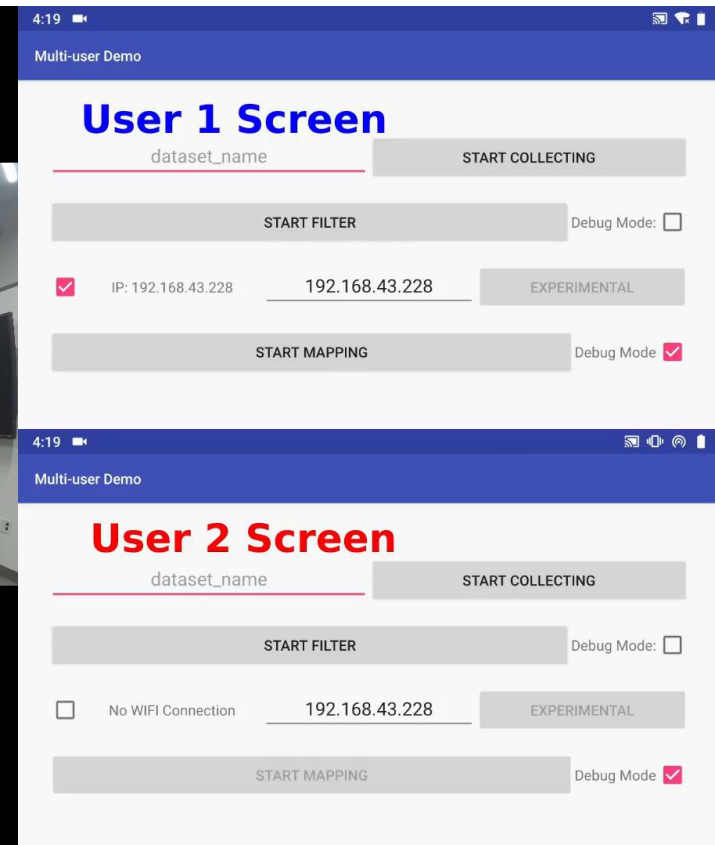
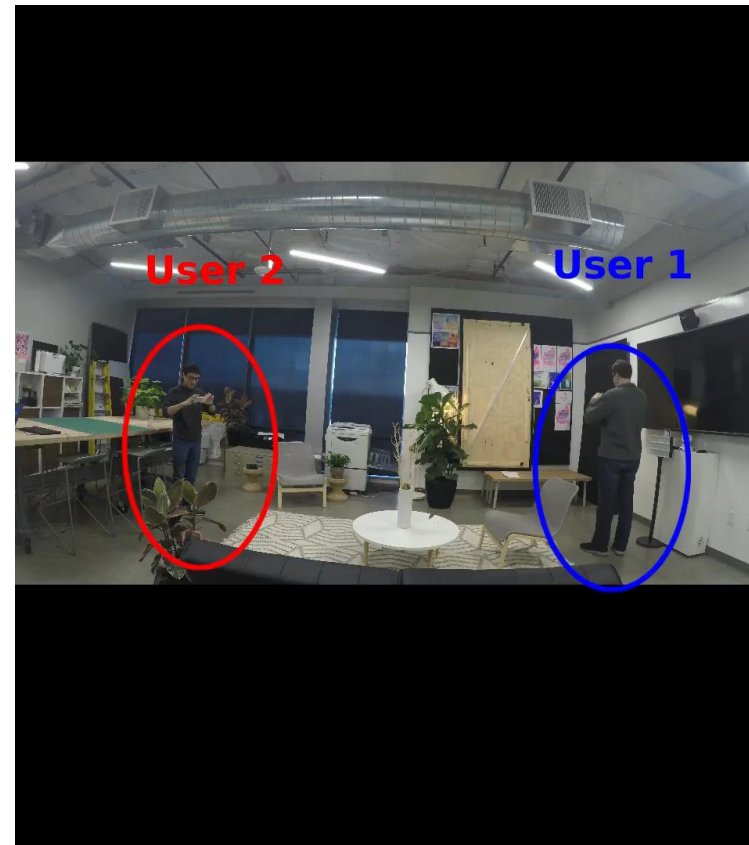
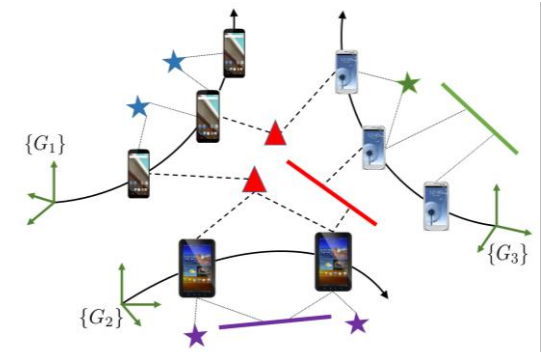


[3] S. Choudhary, L. Carlone, C. Nieto, J. Rogers, H. I. Christensen, and F. Dellaert, "Distributed mapping with privacy and communication constraints: Lightweight algorithms and object-based models," IJRR'17

[4] T. Cieslewski, S. Choudhary, and D. Scaramuzza, "Data-efficient decentralized visual SLAM," ICRA'18

Cooperative VIO/SLAM

- Data from multiple devices are fused to create an area representation
- Centralized [1,2]
 - Computation is offloaded from device
 - Require powerful server for processing
- Distributed [3,4]
 - All devices cooperate to compute a single area representation
- Multi-centralized [5,6,7]
 - Each device computes a map of the area



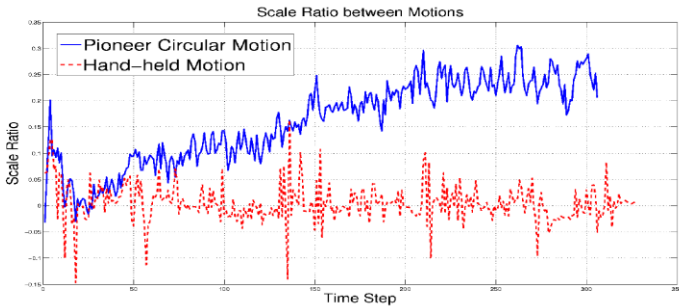
[5] A. Cunningham, V. Indelman, and F. Dellaert, "DDF-SAM 2.0: Consistent distributed smoothing and mapping," ICRA'13

[6] H. Zhang, X. Chen, H. Lu, and J. Xiao, "Distributed and Collaborative Monocular Simultaneous Localization and Mapping for Multi-robot Systems in Large-scale Environments," IJARS'18

[7] K. Sartipi, R. DuToit, C. Cobar, and S. Roumeliotis, "Decentralized Visual-Inertial Localization and Mapping on Mobile Devices for Augmented Reality," IROS'19

Interesting Research Directions

- **Observability Analysis**
 - Additional unobservable directions [1]
 - scale – under const. linear accel.
 - roll, pitch – under const. orientation



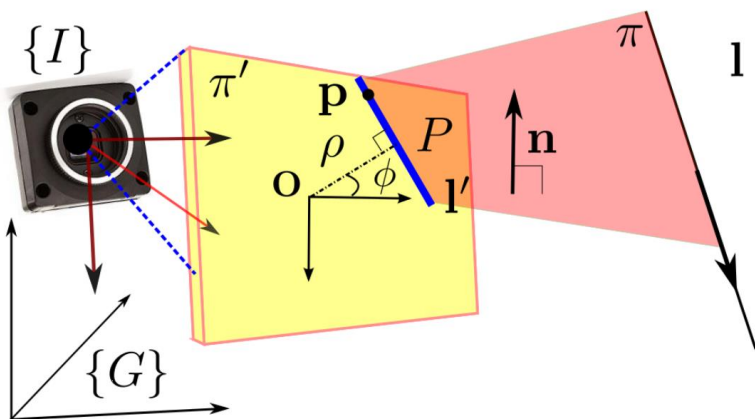
Platform: Pioneer 3 with Google Tango Tablet
Path Length: 1080 m
Total Time: 24 min
Average Speed: 0.7 m/s
Position RMSE: 2.7 m
RMSE/(Path Length): 0.25%

[1] K. J. Wu, C. X. Guo, G. A. Georgiou and S. I. Roumeliotis, "VINS on Wheels", ICRA'17

Interesting Research Directions

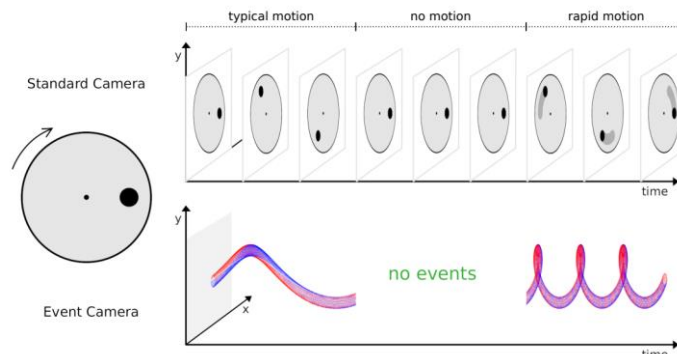
• Observability Analysis

- Additional unobservable directions [1]
 - scale – under const. linear accel.
 - roll, pitch – under const. orientation
- Types of Features: edges, lines, planes [2,3,4]
- IMU/Camera intrinsics, extrinsics, RS, TS



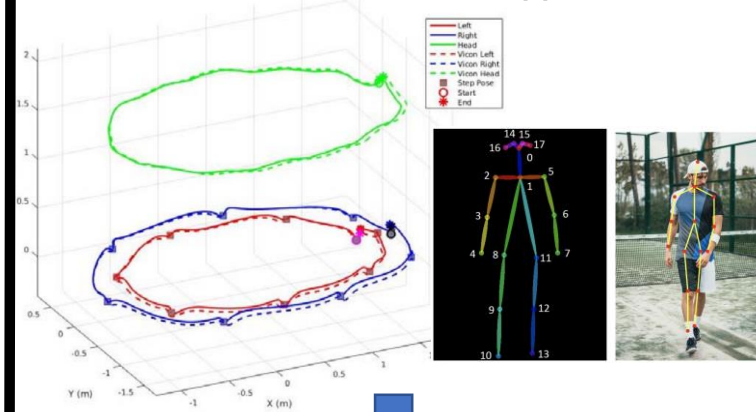
• Event-based camera [5,6]

- Detect changes in intensity, low latency



• Incorporate system's dynamics

- Human motion model [7]



Hybrid, Frame and Event based Visual Inertial Odometry for Robust, Autonomous Navigation of Quadrotors

Antoni Rosinol Vidal, Henri Rebecq, Timo Horstschaefer, Davide Scaramuzza



[1] K. J. Wu, C. X. Guo, G. A. Georgiou and S. I. Roumeliotis, "VINS on Wheels", ICRA'17

[2] D. G. Kottas and Stergios I. Roumeliotis, "Exploiting Urban Scenes for Vision-aided Inertial Navigation," RSS'13

[3] H. Yu and A. I. Mourikis, "Vision-Aided Inertial Navigation with Line Features and a Rolling-Shutter Camera", IROS'15

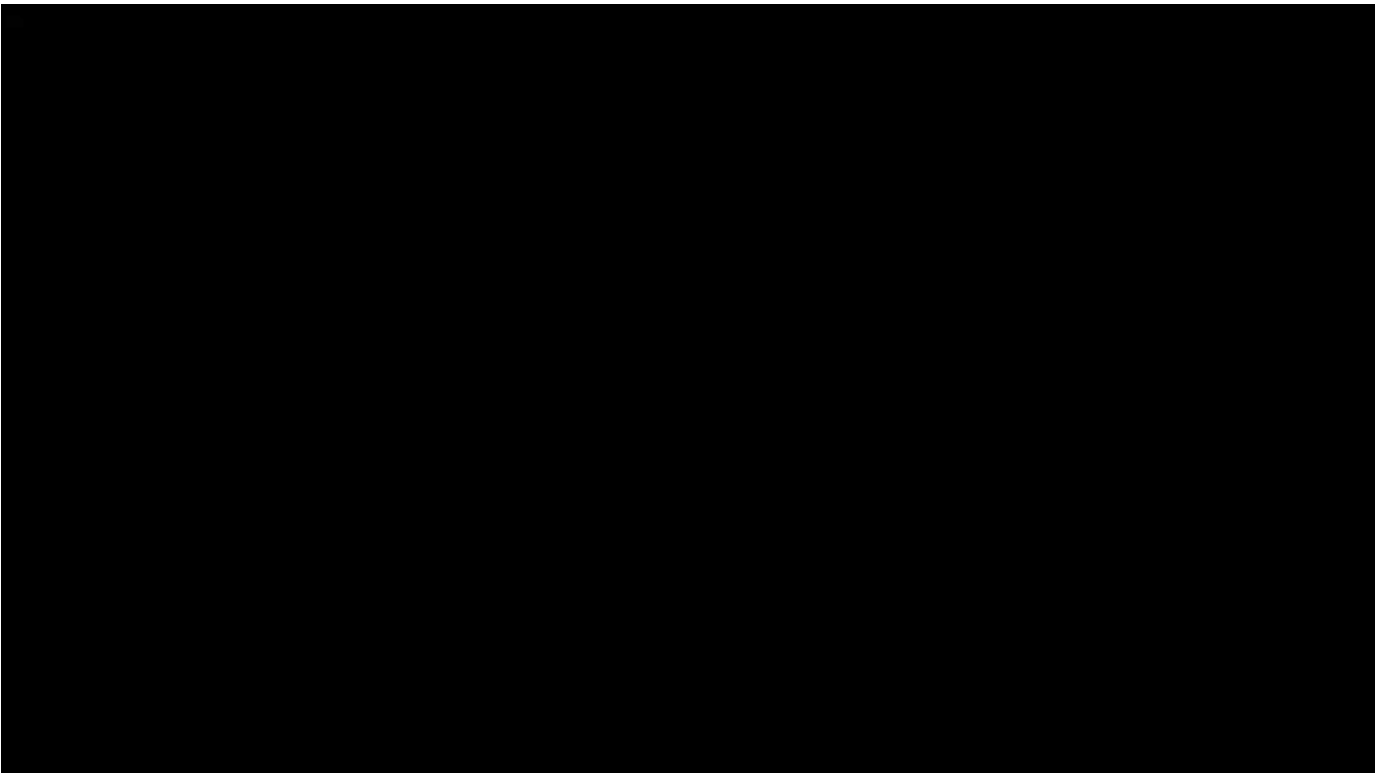
[4] Y. Yang and G. P. Huang, "Aided inertial navigation with geometric features: Observability analysis", ICRA'18

[5] E. Mueggler, G. Gallego, H. Rebecq, D. Scaramuzza, "Continuous-Time Visual-Inertial Odometry for Event Cameras," TRO'18

[6] A. R. Vidal, H. Rebecq, T. Horstschaefer, and D. Scaramuzza, "Ultimate SLAM? Combining Events, Images, and IMU for Robust Visual SLAM in HDR and High Speed Scenarios," RA-L'18

[7] A. Ahmed and S. I. Roumeliotis, "A Visual-Inertial Approach to Human Gait Estimation", ICRA'18

- **Information selection**
 - Geometry based (improve accuracy)
 - Greedy and consider user's intention [1]
 - Heuristics: Long tracks, uniformly distributed, wide baseline, close-by [2]
 - Multi-camera resource allocation [3]



[1] L. Carlone and S. Karaman, "Attention and anticipation in fast visual-inertial navigation," TRO'18

[2] D. G. Kottas, R. C. DuToit, A. Ahmed, C. X. Guo, G. A. Georgiou, R. Li and S. I. Roumeliotis, "A resource-aware vision-aided inertial navigation system for wearable and portable computers," ICRA'14

[3] K. J. Wu, T. Do, L. C. Carrillo-Arce, and S. I. Roumeliotis, "On the VINS Resource-Allocation Problem for a Dual-Camera, Small-Size Quadrotor," ISER'16

- **Information selection**

- Geometry based (improve accuracy)

- Greedy and consider user's intention [1]
- Heuristics: Long tracks, uniformly distributed, wide baseline, close-by [2]
- Multi-camera resource allocation [3]

- Semantic_[4,5] based (improve robustness) exclude ephemeral parts of the scene

moving objects **concern filtering**

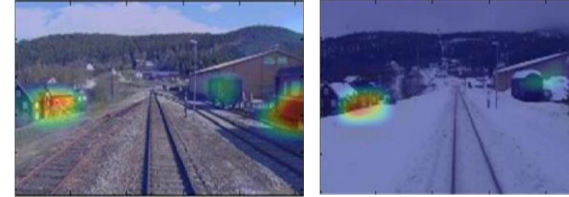


movable objects **concern mapping**

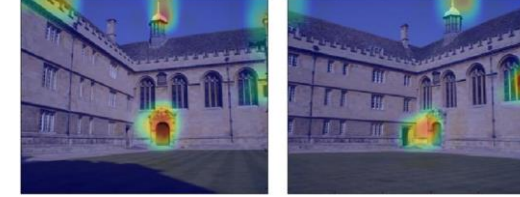


- **Robust scene recognition using ML features** [6]

Season/light Invariance



Viewpoint Invariance



Thank You!



[4] K. He, G. Gkioxari, P. Dollár, and R. Girshick, "Mask RCNN," ICCV'17

[5] T. Pham, T. T. Do, N. Sünderhauf, and I. Reid, "Scenecut: Joint geometric and object segmentation for indoor scenes," ICRA'18

[6] Z. Chen, A. Jacobson, N. Sünderhauf, B. Upcroft, L. Liu, C. Shen, I. Reid and M. Milford, "Deep Learning Features at Scale for Visual Place Recognition," ICRA'17